and its major branches accompanying sustained cellular infiltration in the vessel walls including gamma-delta T cells [3, 4].

Rheumatoid arthritis (RA) is another well-known HLA-associated disease characterized by autoimmunity against synovial membrane and other body components, in which primary association with HLA class II polymorphisms was reported in several different ethnic groups [5]. An additional susceptibility gene for RA was mapped within the same *TNFA-MICB* interval as TA [6]. These observations prompted us to seek a gene or gene polymorphism that may confer the susceptibility to TA and RA within the *TNFA-MICB* interval. The *NFKBIL1* locus is one of several candidates for the susceptible gene near the *C1_2_A* locus, because it encodes for the I kappa B-like (IKBL) protein which has a putative ankyrin repeat sequence and may interact with members of the NF-kappa B/Rel family [7]. As a result, we observed the association of one of the *NFKBIL1* polymorphisms with susceptibility to RA [8]. The association of genetic polymorphism and disease susceptibility is attributed either to direct contribution of the observed genetic alteration to the susceptibility or to linkage disequilibrium (LD) between detected polymorphism and hidden causative genetic alteration(s) of the real disease-susceptibility locus. Accordingly, detailed analysis of haplotype of disease-associated polymorphisms is required.

A genotyping method known as reference strand-mediated conformation analysis (RSCA) has been developed to identify the polymorphisms of several genetic loci including HLA class I [9]. RSCA is based on the double-strand DNA conformation polymorphism of a heteroduplex between a fluorescent dye-labeled "reference" DNA strand and the DNA to be examined. The heteroduplex DNA principally exhibits a unique retardation in mobility upon native polyacrylamide gel electrophoresis according to the number and distribution of mismatched basepairs within the duplex molecule. Therefore, the method is sufficiently robust to detect combinatory difference in DNA sequence such as haplotype of single nucleotide polymorphism (SNP), where the discrimination of genotype is largely dependent on the sequence of the reference DNA strand.

In the present study, we sought candidate polymorphisms for the genetic predisposition to two chronic inflammatory diseases, namely TA and RA, in *NFKBIL1*. As a result, four SNPs in the upstream sequence of the gene were found; −422 $(T)_8/(T)_9$ (eight or nine consecutive thymidines), −325 C/G, −263 A/G, and −63 T/A. Then, we used a method to determine the diplotype, *i.e.*, the combination of haplotypes of these four SNPs for each individual, without family samples by means of RSCA. Consequently, five common SNP haplotypes, or *NFKBIL1* alleles, were observed in the Japanese population, one of which showed a significant association to TA. The TA-associated *NFKBIL1* allele, IKBLp*03, was in strong linkage disequilibrium with C1_2_A*238, which confirmed our previous observation of a risk factor for TA in the HLA region in addition to the HLA-B-linked susceptibility locus. In addition, our analysis revealed that the susceptibility to RA was associated with a different *NFKBIL1* allele, IKBLp*01. To explore the functional relevance of these disease-associated *NFKBIL1* alleles, we examined transcriptional activity of the promoter. We report here that the TA-associated IKBLp*03 showed higher promoter activity than IKBLp*01, suggesting that expressivity of IKBL protein may be differently involved in the predisposition to TA and RA.

MATERIALS AND METHODS

DNA Samples

All study protocols were approved by the Ethics Reviewing Committee of the Medical Research Institute, Tokyo Medical and Dental University. The diagnosis of TA was based on the criteria proposed by the Aortitis Research Group of the Ministry of Health and Welfare, Japan as described previously [10]. The patients with RA were a subset of the patient group enrolled in our previous studies [6, 11] who met the 1987-revised diagnostic criteria of the American Rheumatism Association. Controls were randomly chosen from healthy volunteers representing the Japanese general population. A total of 84 patients with TA [2], 120 patients with RA [6], and 217 healthy control individuals were enrolled in the study. All the patients and control individuals were Japanese and genetically unrelated to each other. DNA was prepared from a blood sample which was obtained from each subject according to given informed consent. HLA and HLA-linked microsatellite polymorphisms were typed as described [2, 6].

Searching for Polymorphisms

PCR–single-strand DNA conformation polymorphism (SSCP) analysis was performed to search for polymorphisms in the promoter and coding region of the *NFKBIL1* gene among 96 individual DNA samples randomly picked up from the controls in the present study, according to the standard method previously described [12]. Primers for the amplification of genomic DNA are listed in Table 1A. Some representative PCR products that manifested different mobility characteristics in the SSCP gel were chosen to be sequenced directly after ExoSAP-IT (Amersham, NJ, USA) treatment. The primer for the direct sequencing reaction was either forward or reverse primer used for amplification.

TABLE 1 Oligonucleotides used in this study

A. Primers for amplification of NFKBIL1 gene

Amplicon	Forward primer	Reverse primer
P3	P3F 5′-TTCCAAACTCCTAAGGGAGG-3′	P3R 5′-TTGTAAGCCCGCAGCTTTGG-3′
P2	P2F 5′-GCCTGGGAGCAGCAGAGACC-3′	P2R 5′-AGACAAAAGACGGAAGAAGAC-3′
P1	P1F 5′-AAATTTTTGCATCTCACTTGCC-3′	P1R 5′-GTTCTTGGCCAGATCTCCC-3′
E1	E1F 5′-CAGACGGCCCCTTTAATTTAAG-3′	E1R 5′-GTCACAGATAATCTCCAATAATG-3′
E2	E2F 5′-CAAGGCTGAAGTCCTGACTG-3′	E2R 5′-GTCAGCTGCTTATGACCTTG-3′
E3	E3F 5′-CTAACTTCTGCTCCCTGCTC-3′	E3R 5′-GGGGAAGGGCAGCTGTGG-3′
E4A	E4AF 5′-ATCACCTTCTCACAGCCTC-3′	E4AR 5′-GGCACATCACCAAATCGCC-3′
E4P	E4PF 5′-AAGAGCACCCCAGAGGAGCG-3′	E4PR 5′-GAGGCTGCAGCCCCGAAGTT-3′

B. Primer for RSCA analysis of NFKBIL1 gene upstream sequence

Forward primer	Reverse primer
P1F 5′-AAATTTTTGCATCTCACTTGCC-3′	E1R 5′-GTCACAGATAATCTCCAATAATG-3′

C. Mutation oligonucleotides[a]

−263mtF	5′-GGCGGGGGAAAAACCTCCA-3′
−263mtR	5′-AGGTTTTTCCCCCGCCTCC-3′
−325mtF	5′-TTCTCTGTGGTTCTCATCTTTTC-3′
−325mtR	5′-GATGAGAACCACAGAGAAAATAGAGG-3′
−63mtF	5′-CTCCACCAAGCGTCTCTGCT-3′
−63mtR	5′-GAGACGCTTGGTGGAGGAC-3′

D. Oligonucleotides for enhancer test constructs[b]

01x2_F	5′-TCGGGGAGGCGGGAAAAAACCTCCGTGGAGGCGGGAAAAAACCTCC-3′
01x2_R	5′-CCGAGGAGGTTTTTTCCCGCCTCCACGGAGGTTTTTTCCCGCCTCC-3′
03x2_F	5′-TCGGGGAGGCGGGGAAAAACCTCCGTGGAGGCGGGGAAAAACCTCC-3′
03x2_R	5′-CCGAGGAGGTTTTTCCCCGCCTCCACGGAGGTTTTTCCCCGCCTCC-3′

E. Primers for real time quantitative PCR

Amplicon	Forward primer	Reverse primer
IKBL	qIF 5′-CGTCGCTTTCGTCGTTACTT-3′	qIR 5′-CCTTGGAGGCATCATCTTCT-3′
GAPDH	qGF 5′-CTTCACCACCATGGAGAAGGC-3′	qGR 5′-GGCATGGACTGTGGTCATGAG-3′

[a] The modified nucleotide is underlined.

[b] Sequences of the 20-bp repeat are underlined.

Cloning and Sequencing of PCR Products

PCR products were ligated to pGEM T-Easy plasmid vector (Promega, WI, USA) and introduced to *Escherichia coli* DH10B competent cells (Invitrogen, CA, USA) according to the manufacturer's instructions. Plasmid DNA was extracted by alkali lysis and subjected to sequencing using the BigDye terminator cycle sequencing kit and ABI 310 automated fluorescent sequencer system (Applied Biosystems, CA, USA).

RSCA of *NFKBIL1* Promoter Polymorphism

A 669-bp *NFKBIL1* gene fragment containing four SNP loci was amplified by PCR under the standard conditions using primers P1F and E1R (Table 1B). The reference strand was prepared by PCR as the amplicon of the 669-bp genomic DNA fragment except for the use of 5′-Cy5-labeled P1F primer instead of ordinary P1F primer. For the modification of the sequence of reference strand, a site-directed mutagenesis by overlap extension PCR was employed [13]. In brief, a pair of mutagenic oligonucleotides for the substitution of G for A at position −262 (relative to the 5′ end of GenBank entry of *NFKBIL1* cDNA, Accession No. X77909) for a plasmid clone derived from PCR of IKBLp*03 was −263mtF/−263mtR (Table 1C). The PCR product of the plasmid DNA template with P1F and −263mtR primers and that with −263mtF and E1R primers were combined and subjected to ligation-PCR using flanking primers, P1F and E1R. Similarly, an insertion of G at −325 and

an insertion of T at −63 were introduced into a plasmid clone of IKBLp*04 using two pairs of mutagenic oligonucleotides; −325mtF/−325mtR and −63mtF/−63mtR, respectively (Table 1C). Then, these two mutant DNA clones were cut with restriction enzyme *Bgl*II and ligated to combine both modified sites.

Heteroduplexes were formed by the addition of 1 μl of reference PCR product (200–300 ng/μl) to 3 μl of test PCR product (200–300 ng/μl) followed by denaturating at 95°C for 4 minutes, annealing at 55°C for 5 minutes, and cooling down to 15°C for 5 minutes; 6x Ficoll loading dye (15% Ficoll, 0.25% bromophenol blue) and internal standards for the mobility (519-bp and 870-bp Cy5-labeled DNAs) were added after duplex formation. Samples were separated by electrophoresis in a nondenaturing 6% Long Ranger polyacrylamide gel (Biowhittaker Molecular Applications, ME, USA)/1×TBE buffer (89 mM Tris, 89 mM boric acid, and 2 mM EDTA, pH 8.0) on ALFexpress Sequencer/Fragment Analyzer (Pharmacia Biotech, Uppsala, Sweden) at 30 W constant power. The gel temperature was maintained at 40°C during electrophoresis. The mobility of each fluorescent fragment was analyzed by Fragment Manager Software (Pharmacia Biotech).

Statistical Analysis

The frequencies of each allele, each genotype, and carrier for each allele in the patient group were compared with those in the control group. The strength of the association was expressed by the odds ratio (OR) and statistical significance was examined by Fisher's exact test using R statistical package. Interval estimate for OR was obtained according to the literature [14]. The p values of the OR were further corrected for multiple statistical tests by multiplying with the number of *NFKBIL1* promoter alleles ($n = 5$) found in the Japanese population. When the corrected p value (p_c) was less than 0.05, the association was considered to be significant.

Analysis of Linkage Disequilibrium

LD between *NFKBIL1* promoter allele and HLA polymorphism was assessed by calculating normalized LD coefficient (D′) [15] and correlation coefficient (r^2) [16] following the estimation of haplotype frequency of the control population from individual data set by means of EH program obtained from Web resource at the Rockefeller University (http://linkage.rockefeller.edu/ott/eh.htm). Significance of LD was evaluated using the value of minus twice the logarithm of likelihood ratio under assumptions of presence and absence of LD which is known to approximately follow a χ^2 distribution with one degree of freedom [17].

Stratification Analysis

To examine the interaction between IKBLp polymorphism and HLA-B allele, the risk conferred by IKBLp polymorphism was evaluated by the value of OR when the patients and controls were classified into subgroups by the presence or absence of a certain HLA-B allele and vice versa [18].

Functional Analysis of *NFKBIL1*-263 Polymorphism

To explore whether −263G/A polymorphism can contribute to the difference in transcriptional enhancer activity, we constructed a series of oligomeric tandem repeats of the 20-bp-long sequence around the SNP (−272 to −253) ligated with a basal promoter derived from adenovirus E1B gene [19]. In brief, a double-strand DNA containing two copies of the repeats corresponding either to −263G or to −263A allele was made by annealing of oligonucleotides 01×2_F and 01×2_R or 03×2_F and 03×2_R (nucleotide sequences are listed in Table 1D). Then it was inserted into the nonsymmetrical cohesive ends of pUC0OCAT cleaved with *Ava*I restriction enzyme as a monomer or head-to-tail ordered oligomers [20]. The repeats were cut *en bloc* after transformation of *dcm* mutant *E. coli* host (BL21) with *Apa*I and *Bam*HI and inserted at an upstream position of E1B TATA box cloned in the pGL3-basic firefly luciferase reporter plasmid (Promega). The enhancer activity was measured by relative luciferase activity upon the transfection. Raji cells (1×10^6) were transfected with a mixture of the luciferase reporter and a Renilla luciferase reporter plasmid pRL-tk by using Trancfectin (Bio-Rad). The cell lysate was collected at 24 hours after transfection. The promoter activity was measured as relative light intensity of reporters with Dual Luciferase assay kit (Promega) by using Luminous CT-9000 luminometer (DIAIatron, Germany).

Promoter Assay

The 1204 bp-long *NFKBIL1* gene fragment spanning from −1182 to +82 was amplified by PCR using primers P3F and E1R. The resultant DNA fragment corresponding to each of five alleles (IKBLp*01 through *05) was ligated to pGL3-basic plasmid in which was the firefly luciferase reporter to be driven by the inserted DNA upon the transfection to Raji cells, as described above. The assays were performed with six different preparations of reporter plasmid DNA for each of five constructs to take into account a possible variation in quality among different preparations of plasmid DNA. The data were analyzed with one-way ANOVA.

TABLE 2 Genotype of IKBLp and HLA-A, -B, and -DRB1 loci of B-lymphoblastoid cell lines

Name	IHWC number	IKBLp[a]	HLA-A	HLA-B	HLA-DRB1	HLA homozygosity[b]
TUBO	IHW 9045	*01/*01	*0216/*0301	*5101	*1104/*1201	HLA-A, DRB1 heterozygote
BM16	IHW 9038	*01/*01	*0201	*1801	*1201	yes
RML	IHW 9016	*01/*01	*0204	*5101	*1602	yes
SA	IHW 9001	*02/*02	*2402	*0702	*0101	yes
HHKB	IHW 9065	*02/*02	*0301	*0702	*1301	yes
MGAR	IHW 9014	*02/*02	*2601	*0801	*1501	yes
Akiba	IHW 9286	*03/*03	*2402	*5201	*1502	yes
HY969	not applicable	*03/*03	*2402	*5201	*1502	yes
TOK	not applicable	*03/*03	*2402	*5201	*1502	yes
BM21	IHW 9043	*05/*05	*0101	*4101	*1101	yes
TAB069	IHW 9066	*05/*05	*0201/*0207	*4601	*0803	HLA-A heterozygote
KAS116	IHW 9003	*05/*05	*2402	*5101	*0101	yes

[a] Genotype of IKBLp was confirmed by nucleotide sequencing.

[b] All the cell lines were derived from HLA-B homozygotes. They were also homozygous for HLA-A and DRB1 loci otherwise mentioned.

Culture of Genotype-Defined Cells and Quantification of *NFKBIL1* Transcript

HLA-defined B lymphoblastoid cell lines homozygous for four of five IKBLp alleles (Table 2) were cultured in RPMI medium 1640 supplemented with 10% fetal bovine serum under 5% CO_2. Cells were collected at growing phase and approximately 10^7 cells were subjected to total cellular RNA preparation by RNeasy mini kit (Qiagen). One microgram of RNA was used to synthesize cDNA by Superscript II reverse transcriptase (Invitrogen) according to the manufacturer's instruction. Quantitative real-time PCR used iCycler iQ Real-Time PCR Detection System (Bio-Rad) and iQ SYBR Green Supermix kit (Bio-Rad) to measure relative amount of mRNA. Primers for quantification of *NFKBIL1* and *GAPDH* transcripts are listed in Table 1E. Relative amount of *NFKBIL1* transcript was divided by that of *GAPDH*, a well-known housekeeping gene, for standardization.

RESULTS

Polymorphisms of *NFKBIL1* Locus

Our previous study mapped one of the susceptibility loci for TA around the 70-kb-long interval between the *TNFA* and the *MICB* loci of the HLA region [2], which was identical to the susceptibility locus for RA [6]. There are six functional genes in this interval; *TNFA, LTA, NFKBIL1, ATP6G, BAT1,* and *MICB.* We then searched for polymorphisms of *NFKBIL1* gene as a candidate genetic risk for TA, because an *NFKBIL1* polymorphism was associated with the susceptibility to RA [8]. By the screening of 96 healthy Japanese individuals by SSCP and subsequent sequencing analysis, we could not find polymorphism in the protein coding sequence, but there were four polymorphic sites in the 5′-flanking region of the gene which were registered in the dbSNP database with the ID numbers in parentheses: eight or nine consecutive thymidines $(T)_8/(T)_9$ at position −422 (rs3219186, rs9279341), C/G at position −325 (rs3219185), A/G at position −263 (rs3219184), and T/A at position −63 (rs2071592). Sequencing of 669 (or 670)-nucleotide-long inserts of PCR-derived clones that contained all four sites revealed that the combinations of four SNPs fell into only five types of 16 possible combinations. We designated these five types of *NFKBIL1* promoter alleles IKBLp*01 through IKBLp*05 (IKBLp*01, co-occurrence of $-422(T)_8$, −325C, −263A, and −63T; IKBLp*02, co-occurrence of $-422(T)_9$, −325C, −263A, and −63T; IKBLp*03, co-occurrence of $-422(T)_8$, −325C, −263G, and −63T; IKBLp*04, co-occurrence of $-422(T)_8$, −325G, −263A, and −63A; and IKBLp*05, co-occurrence of $-422(T)_8$, −325C, −263A, and −63A) (Figure 1).

Development of RSCA-Based Typing Method for *NFKBIL1* Promoter

Because the alleles of *NFKBIL1* promoter were defined as a combination of the four SNPs, we attempted to develop a typing method to determine the alleles directly by RSCA. The sensitivity of sequence discrimination upon RSCA is dependent on the sequence of the reference strand so that it can be improved empirically by mutagenesis of the reference strand. Generally, a mispairing caused by insertion/deletion mutation or mismatches in two or more consecutive positions causes a greater effect on the mobility of the heteroduplex than that caused by a single base substitution. Therefore, we expected that introducing a mutation at or near the SNP site would improve the allele discrimination. When we used a native IKBLp*04 sequence as a reference to make a duplex with cloned DNA, mobility of each duplex was similar to the others except for the heteroduplex with IKBLp*02

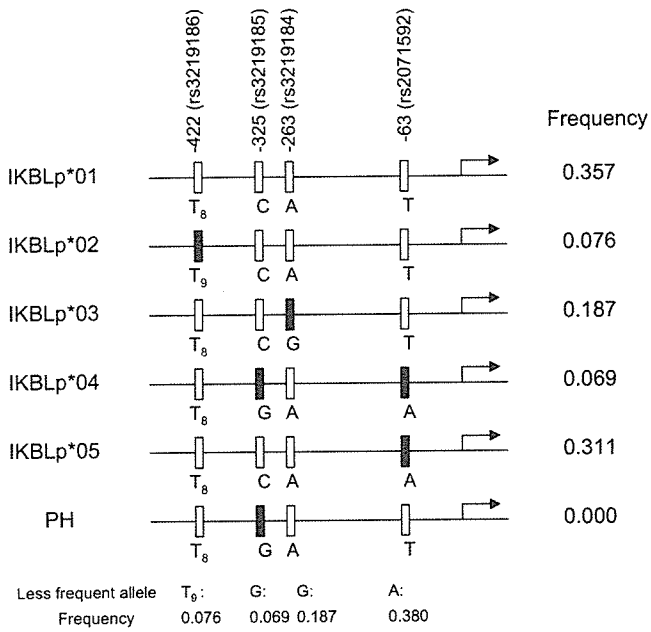

FIGURE 1 Schematic illustration of the *NFKBIL1* promoter alleles. Five of 16 possible combinations of four SNPs were commonly found in Japanese, and designated IKBLp*01 through *05. Frequency of each combination in the general population is at the right of the scheme. Ref SNP ID and frequency of less frequent allele for each SNP are also presented. A molecular clone corresponding to the bottom one (PH), which has not yet been identified, was made artificially to test the performance of the typing method.

which possessed a mismatch of one base insertion/deletion (Figure 2A, left). An insertional mutation of G at −325G of IKBLp*04 produced remarkable changes in the mobility of duplexes with the −325C alleles (Figure 2A, center). In addition, insertion of A at −63 brought an enhancement in discrimination of IKBLp*05 from the others (Figure 2A, right). Similarly, IKBLp*03 was mutagenized at −263. During the isolation of reference DNA in the plasmid, an unexpected base change took place at −422 which helped to separate the homoduplex signal and heteroduplex signals (Figure 2B). The final set of the reference strands was "Ref-1" with a deletion of T at −422 and an A to G change at −262 introduced in IKBLp*03 sequence and "Ref-2" with an insertion of G at −325 and an insertion of A at −63. With Ref-1, the IKBLp*01 and IKBLp*03 could be uniquely distinguished from the other alleles (Figure 2B, right), whereas the discriminations of IKBLp*04 and IKBLp*05 were apparent with Ref-2. Using these two reference strands in combination, all five alleles can be identified without ambiguity.

An advantage of RSCA over the individual SNP genotyping was an ability to resolve "haplotypic" or *cis–trans* ambiguities. For example, when the genotype of these four SNPs is homozygous for $(T)_8$ at −422 ($(T)_8/(T)_8$), heterozygous at −325 (C/G), homozygous for A at −263 (A/A), and heterozygous at −63 (T/A), one cannot determine whether the haplotypic combination of these SNPs is heterozygous for IKBLp*01 ($(T)_8$-C-A-T) and IKBLp*04 ($(T)_8$-G-A-A) or heterozygous for IKBLp*05 ($(T)_8$-C-A-A) and a possible haplotype $(T)_8$-G-A-T ("PH" in Figure 1, so far not identified in Japanese). The electrophoretic patterns with these two genotypes were clearly different as demonstrated in Figure 2C.

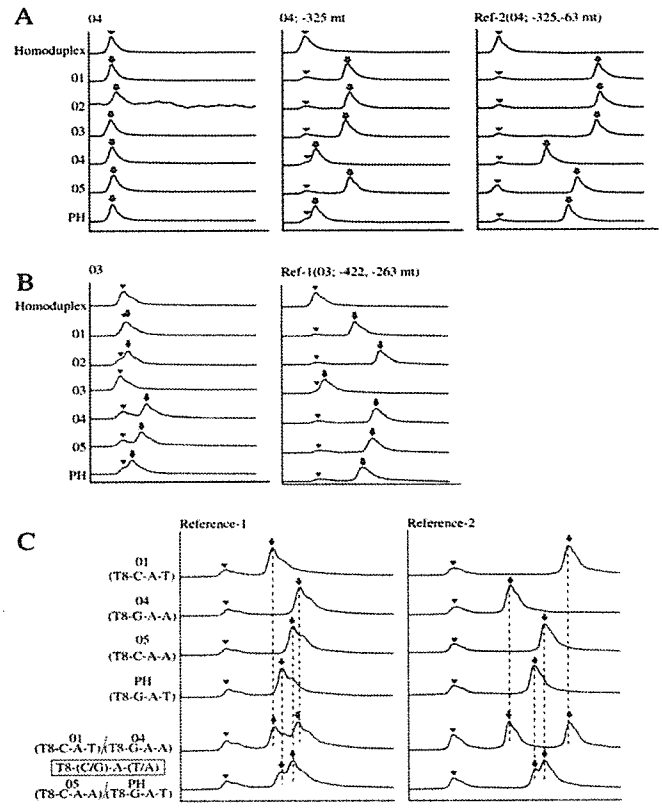

FIGURE 2 Effect of mutations of the references on the allele discrimination of RSCA. Different reference strands were tested for discrimination of the *NFKBIL1* promoter alleles. PCR products derived from plasmid clones of five common alleles and an unidentified combination $(T)_8$-G-A-T, tentatively assigned to PH, were examined. (A) Native IKBLp*04 (left), a mutant at position −325 (middle), and a double mutant at positions −325 and −63 (right, named Ref-2) were examined. Homoduplex of the reference is indicated by arrow head, and heteroduplex is indicated by arrow. (B) Native IKBLp*03 (left) and a double mutant at positions −422 and −263 (right, named Ref-1). (C) Resolution of *cis–trans* ambiguity of compound heterozygote for SNPs. PCR products were mixed to mimic heterozygote samples, *01/*04 and *05/PH. RSCA clearly resolved these genotypes, which fall on the same combination of individual SNP genotype: $(T)_8/(T)_8$-C/G-A/A-T/A.

TABLE 3A Association of IKBL polymorphism to Takayasu's arteritis

IKBLp allele	Carriers in patients (n = 84)	Carriers in control (n = 217)	Odds ratio (95% CI)	p	pc
IKBLp*01	38 (45.2%)	126 (58.1%)	0.60 (0.36–1.00)	n.s.[a]	n.s.
IKBLp*02	8 (9.5%)	33 (15.2%)	0.59 (0.26–1.33)	n.s.	n.s.
IKBLp*03	48 (57.1%)	76 (35.0%)	2.47 (1.45–4.14)	0.00065	0.0032
IKBLp*04	10 (11.9%)	30 (13.8%)	0.84 (0.39–1.81)	n.s.	n.s.
IKBLp*05	42 (50.0%)	109 (50.2%)	0.99 (0.60–1.64)	n.s.	n.s.

[a] Not significant; p or $pc > 0.05$.

Analysis of *NFKBIL1* Promoter Alleles in TA

We examined 84 TA patients. The frequency of IKBLp*03 was significantly increased in the patients compared to that in the controls, 57.1% vs 35.0%, odds ratio of risk (OR) = 2.47, p_c = 0.0032, indicating that this allele was strongly associated with the susceptibility to TA (Table 3A). Because −263G SNP is unique to IKBLp*03 among the five common alleles, these findings suggest that −263G SNP is a promising candidate for the responsible polymorphism controlling the susceptibility to TA.

Analysis of *NFKBIL1* Promoter Alleles in RA

We have previously reported that −63T SNP was strongly associated with RA in Japanese [8]. To examine the association further at the allele level, we used the RSCA-based typing method to analyze 120 patients with RA. As shown in Table 3B, the frequency of IKBLp*01 was increased in the RA patients; 73.3% vs 58.1%, OR = 1.99, p_c = 0.032, whereas the frequencies of the other −63T-bearing *NFKBIL1* alleles, IKBL*02 and IKBLp*03 (Figure 1), were not increased. Although the results were consistent with −63T being strongly associated with RA, it was suggested that not the presence of the −63T SNP alone but the specific haplotypic combination of *NFKBIL1* promoter polymorphisms may confer the susceptibility to RA.

Linkage Disequilibrium of *NFKBIL1* Promoter Alleles with HLA

Because significant extent of LD between alleles of the genes in the HLA region had been observed, we next examined LD between *NFKBIL1* alleles and other polymorphisms in the HLA region in the control population. We found that several alleles of genes in the HLA region manifested significant LD with five common *NFKBIL1* alleles as listed in Table 4 It was of note that significant LD was observed in a rather expanded region of the genome encompassing over a few megabases (from HLA-A to HLA-DPB1) when D′ was used as an index of LD. We considered that this was due to the multiallelic nature of HLA loci and microsatellite markers and that the observations were in accordance with the concept of "HLA ancestral haplotypes" [21]. The frequencies of alleles were generally low so that LD could be captured by the analysis with D′, whereas another index for LD, r^2, was not necessarily high between alleles of distant loci.

With regard to the TA-associated alleles, microsatellite alleles TNFd*134, C1_2_A*238, TNFa*119, and MICA(GCT)n*A6 were in strong LD with IKBLp*03, which was in good accordance with the TA-associated *NFKBIL1* allele being identified in our previous study [2] as a genetic variation linked to C1_2_A*238. B*5201 was also in strong LD with IKBLp*03 (D′ = 0.828, r^2 = 0.464) with an estimated haplotype frequency of 0.119, which was the most frequent *NFKBIL1-HLA-B* haplotype in Japanese. Because of strong LD between IKBLp*03 and B*5201, one may assume that either of them was truly associated with TA and that the other had no effect on the disease susceptibility but merely increased in frequency as the carriers of *NFKBIL1-HLA-B* haplotype were increased in patients. Then, we analyzed the interaction between the disease-associated alleles by stratifying the population by the presence or absence of the alleles at risk (Table 5). IKBLp*03 increased the risk from OR of 2.54 to 6.98 in

TABLE 3B Association of IKBL polymorphism to rheumatoid arthritis

IKBLp allele	Carriers in patients (n = 120)	Carriers in control (n = 217)	Odds ratio (95% CI)	p	pc
IKBLp*01	88 (73.3%)	126 (58.1%)	1.99 (1.22–3.23)	0.0065	0.032
IKBLp*02	16 (13.3%)	33 (15.2%)	0.86 (0.45–1.63)	n.s.[a]	n.s.
IKBLp*03	36 (30.0%)	76 (35.0%)	0.80 (0.49–1.28)	n.s.	n.s.
IKBLp*04	8 (6.7%)	30 (13.8%)	0.45 (0.20–1.00)	0.049	n.s.
IKBLp*05	52 (43.3%)	109 (50.2%)	0.76 (0.48–1.19)	n.s.	n.s.

[a] Not significant; p or $pc > 0.05$.

TABLE 4 Linkage disequilibria between IKBL polymorphisms and alleles of genetic markers in the HLA region

Markers	IKBLp*01	IKBLp*02	IKBLp*03	IKBLp*04	IKBLp*05
HLA-A			*2402 (0.460,0.073)	*3303 (0.764,0.542)	*0207 (0.791,0.063)
C3_2_11		*227 (0.799,0.326)	*207 (0.548,0.246)	*197 (0.782,0.158)	
C2_4_4	*251 (0.689,0.044)	*231 (0.854,0.053)	*243 (0.751,0.404)	*259 (0.751,0.300)	*255 (0.575,0.104)
C1_3_1	*279 (0.596,0.063)	*293 (0.623,0.254)	*291 (0.618,0.262)	*291 (0.890,0.184)	*288 (0.768,0.214)
C1_2_5	*192 (0.685,0.048)	*200 (0.619,0.169)	*208 (0.752,0.383)	*218 (0.799,0.425)	*194 (0.692,0.036)
HLA-B	*3901 (0.819,0.032)	*0702 (0.911,0.637)	*5201 (0.828,0.464)	*4403 (0.887,0.759)	*1501 (0.665,0.092)
	*5401 (0.694,0.068)		*6701 (0.999,0.066)		*4601 (0.876,0.130)
	*3501 (0.821,0.073)				
C1_4_1	*213 (0.396,0.040)	*225 (0.678,0.380)	*217 (0.672,0.104)	*217 (0.706,0.039)	
	*221 (0.354,0.060)				
	*229 (0.750,0.066)				
MIB	*344 (0.741,0.046)	*336 (0.644,0.227)	*326 (0.528,0.124)	*336 (0.870,0.372)	*326 (0.216,0.040)
	*346 (0.624,0.166)				
MICA (GCT)n	A4 (0.677,0.152)	A5.1 (0.798,0.297)	A6 (0.685,0.283)	A6 (0.883,0.160)	A5 (0.542,0.287)
	A9 (0.458,0.039)				
C1_2_A	*242 (0.521,0.152)	*242 (0.628,0.103)	*238 (0.771,0.294)	*236 (0.854,0.114)	*236 (0.696,0.414)
	*250 (0.611,0.035)				
	*256 (0.487,0.047)				
TNFa	*95 (0.999,0.043)	*115 (0.750,0.244)	*119 (0.892,0.731)	*105 (0.921,0.121)	*105 (0.839,0.570)
	*97 (0.965,0.261)				
	*113 (0.793,0.124)				
LTA A252G	252A (1.000,0.338)	252A (0.999,0.051)	252A (0.925,0.119)	252G (0.905,0.106)	252G (1.000,0.717)
TNFA promoter	*B (0.966,0.287)	*A (0.999,0.048)	*A (1.000,0.130)	*A (0.999,0.042)	*A (0.853,0.169)
	*C (1.000,0.036)				
	*D (0.943,0.330)				
TNFd	*130 (0.519,0.264)	*130 (0.925,0.123)	*134 (0.782,0.206)	*132 (0.910,0.361)	*134 (0.487,0.154)
					*138 (0.929,0.129)
D6S273		*132 (0.648,0.151)	*136 (0.522,0.194)	*136 (0.834,0.169)	*134 (0.267,0.065)
HLA-DRB1	*0405 (0.604,0.094)	*0101 (0.842,0.614)	*1502 (0.763,0.461)	*1302 (0.909,0.674)	*0803 (0.395,0.038)
HLA-DQA1	*0302 (0.294,0.075)	*0101 (0.842,0.614)	*0103 (0.499,0.171)	*0102 (0.789,0.341)	
DQ-CARII		*201 (0.703,0.461)	*205 (0.436,0.141)	*207 (0.842,0.502)	*203 (0.999,0.034)
HLA-DQB1	*0401 (0.593,0.088)	*0501 (0.809,0.589)	*0601 (0.479,0.166)	*0604 (0.952,0.683)	*0302 (0.474,0.040)

Alleles of genetic markers in the HLA region that showed significant linkage disequilibria (LD) with each IKBL promoter allele are shown. LD values (D′ and r^2) are indicated in parentheses. Allele definitions follow those in the literature [2,29].

the presence of B*5201, although this was not statistically significant because both patients and controls in columns were decreased by stratification. It was also observed for the risk conferred by B*5201 in the presence of IKBLp*03 (OR increase from 2.91 to 3.36), and in this case statistical significance was obtained. Accordingly, both IKBL*03 and B*5201 were suggested to be truly associated with TA.

Functional Analysis of the *NFKBIL1* Promoter Polymorphism at −263

Because the polymorphism of *NFKBIL1* was found in the upstream sequence, the risk for TA or RA would be attributed to the difference in the regulation of gene expression. Thus the promoter activity was examined by the luciferase reporter system. Since IKBLp*03 was unique at

TABLE 5 Stratification analysis to access the HLA-B-linked and IKBLp-linked risks for Takayasu's arteritis

Population	Allele at risk	Carriers/noncarriers		OR (95% CI)	p
		In patients	In controls		
Unstratfied	IKBLp*03	48/35	74/137	2.54 (1.51–4.27)	0.00058
	B*5201	42/41	55/156	2.91 (1.71–4.93)	0.00010
B*5201 carriers	IKBLp*03	41/1	47/8	6.98 (0.84–58.18)	n.s.[a]
B*5201 noncarriers	IKBLp*03	7/34	27/129	0.98 (0.39–2.45)	n.s.
IKBLp*03 carriers	B*5201	41/7	47/27	3.36 (1.32–8.54)	0.012
IKBLp*03 noncarrier	B*5201	1/34	8/129	0.47 (0.06–3.92)	n.s.

[a] Not significant: $p > 0.05$.

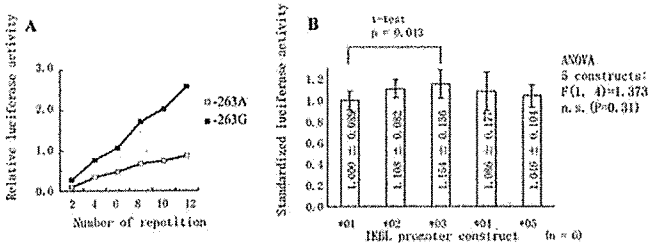

FIGURE 3 Functional analysis of *NFKBIL1* promoter. (A) A series of enhancer test constructs with variable numbers of 20-bp repeats containing −263 SNP were made by inserting the multimer of oligonucleotide upstream of adenoviral E1B basal promoter and tested for the transcriptional activity. The firefly luciferase activity was measured and standardized by *Renilla* luciferase activity driven by HSV thymidine kinase promoter. Numbers on *x* axis indicate the repetition of 20-bp sequence. (B) Nucleotide sequence encompassing −1182 to +23 of five alleles (IKBLp*01 through *05) were examined for transcriptional activity. Bar graph shows mean ± standard error of the mean (n = 6). A test with one-way ANOVA did not demonstrate unevenness of activity among five constructs with statistical significance ($F(1,4)$ = 1.37, p = 0.31).

−263, we focused on this point. We compared transcriptional enhancer activity of −263G and −263A SNP alleles. For this purpose, a series of multimers of sequence containing either −263G or −263A was inserted upstream of E1B TATA promoter and the resultant plasmids were transfected to Raji B lymphoblastoid cells, in which *NFKBIL1* gene was expressed [our unpublished observation]. The transfectants were assayed for luciferase activity. As shown in Figure 3A, −263G, characteristic SNP of IKBLp*03, showed higher driving activity on E1B TATA promoter consistently, suggesting that IKBL*03 may manifest higher transcriptional activity than the other alleles.

To further corroborate the difference in transcriptional activity, we compared the promoter activity of the region spanning from −1182 to +82 of all five kinds of IKBLp alleles (Figure 3B). Althogh one-way ANOVA indicated that the experiment failed to demonstrate the significant unevenness in the transcriptional activity among five promoter alleles ($F(1,4)$ = 1.37, p = 0.31), only the comparison between IKBLp*01 and IKBLp*03 constructs reached statistical significance (p = 0.043) by Student's t-test among ten possible pairwise comparisons. These results raised the possibilities that the augmented expression of *NFKBIL1* gene or IKBL protein may be involved in the predisposition to TA and that the lower expression may be involved in the predisposition to RA.

Effect of NFKBIL1 Promoter Polymorphism on the Amount of Transcripts

The difference in promoter activity may lead to the difference in the amount of transcript in the cells. We examined the steady state mRNA levels of *NFKBIL1* in B lymphoblastoid cell lines derived from homozygotes of IKBLp*01, ILBLp*02, ILBLp*03, and ILBLp*05 (Table 2, Figure 4). The amount of *NFKBIL1* mRNA standardized by GAPDH mRNA among 12 different cell lines varied significantly (one-way ANOVA, $F(1,11)$ = 10.82, p = 0.0072), while the variation within each of four groups of three cell lines with the same genotype was not significant. Thus, one of the major factors for the variation was the difference in *NFKBIL1* genotype. Post hoc analysis of comparison between genotypes revealed the consistent tendency of lower expression level in IL-BLp*01 compared to levels in the others. The results were in good concordance with functional studies and reinforced the notion that the augmentation and attenuation of *NFKBIL1* gene expression may contribute to the susceptibility for TA and RA, respectively.

DISCUSSION

In this study, we developed an RSCA-based typing method for *NFKBIL1* gene and applied it to the associ-

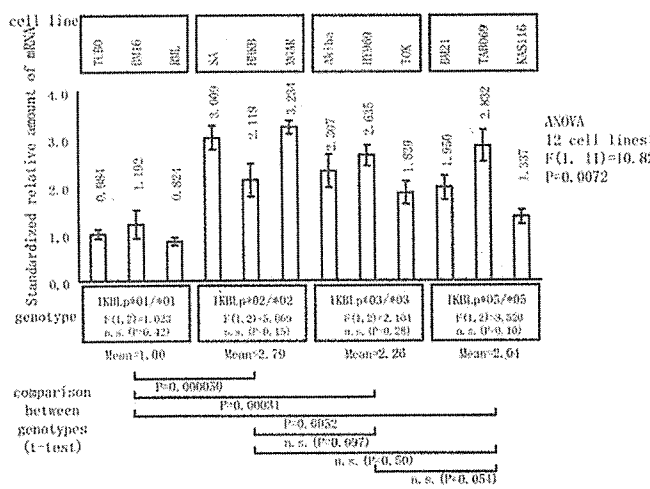

FIGURE 4 Quantification of *NFKBIL1* mRNA. Bar graph shows mean ± standard error of the mean of standardized relative amount of *NFKBIL1* mRNA (n = 3). Genotype of each cell line is listed in Table 2. The values were obtained by dividing the relative amount of *NFKBIL1* mRNA by the relative amount of *GAPDH* mRNA in the same sample and normalizing the mean value of three IKBLp*01 homozygotes to be 1.00. One-way ANOVA demonstrated that the amount of RNA among 12 cell lines was different ($F(1,11)$ = 10.82, p = 0.0072), although every three cell lines with the same genotype did not vary. $F(1,2)$ values were 1.013, 5.073, 2.106, and 8.520 which corresponded to p values of 0.42, 0.15, 0.28, and 0.10, respectively, for IKBLp*01/*01, *02/*02, *03/*03, and *05/*05. Post hoc analysis of comparison between mean standardized relative amounts of mRNA of respective genotypes revealed that the smaller amount of *NFKBIL1* mRNA associated with IKBLp*01/*01 genotype.

ation analysis of the susceptibility to TA and RA. RSCA had been shown to be useful for determining genotypes of complicated polymorphic loci such as the HLA genes [9]. In the course of the development, we found that introducing insertion/deletion mutation at or near the polymorphic nucleotide to be determined facilitated the allelic discrimination by the mobility shift of heteroduplex DNA. This finding would be helpful in designing a new RSCA assay for genotyping of other gene polymorphisms. The RSCA-based typing of *NFKBIL1* was accurate because we did not see any discrepancy between RSCA typing data and SNP typing data of 116 RA samples which had been used in the previous study [8] or between RSCA typing data and SSCP typing data of 96 controls described above. RSCA is also useful for the discovery of polymorphism because any difference in the sequence has a possibility to result in the molecular conformation change as in the SSCP analysis. In fact, during the association study of TA, we found an individual with aberrant pattern of RSCA who turned out to have a novel SNP of C for G at +63.

We observed an association of IKBLp*01 with RA. This was in part a confirmative result of the association between RA and −63T of *NFKBIL1*. However, since IKBLp*02 and IKBLp*03, both of which carried −63T, did not show the association, our findings clearly indicated that −63T solely could not confer the susceptibility to RA. On the other hand, the observed association of IKBLp*03 allele with TA was in a good accordance with our previous observation of the association between TA and a microsatellite allele C1_2_A*238, because IKBLp*03 and C1_2_A*238 were in strong LD in the Japanese population. In addition to HLA-B*5201, HLA-B*3902 and HLA-B*6701 were associated with TA [1]. Although the number of samples was not sufficient to demonstrate the statistical significance for B*3902, these three HLA-B alleles were commonly in LD with IKBLp*03. So it is possible that the association of HLA-B alleles with TA may reflect a LD between these alleles and IKBLp*03. However, it was not the case because the stratification analysis demonstrated that both IKBLp*03 and HLA-B alleles separately contributed to the risk at least for HLA-B*5201 (see Results).

IKBLp*03 carries a unique sequence of G at −263, suggesting that this SNP would be responsible for the susceptibility to TA. We could demonstrate the difference in promoter activity with the SNP by luciferase reporter assays. TFSEARCH program (http://mbs.cbrc.jp/research/db/TFSEARCH.html) revealed that the sequence around −263A forms a putative E2F binding site [22], whereas that around −263G matched a putative c-Rel binding site [23] at default setting of threshold (85%). Thus transcriptional regulation of the alleles might be different by change in sequence with −263A/G polymorphism. Recently, several reports on disease association of *NFKBIL1* promoter polymorphism were published to support the notion that *NFKBIL1* was a regulator gene for autoimmunity; *NFKBIL1* promoter with −263G and −63T, that is IKBLp*03, was associated with the resistance to type I diabetes [24].

Tissue distribution of *NFKBIL1* mRNA, data for which was not presented here, was somewhat different from that of mouse homologue [20]. *NFKBIL1* mRNA was detected in a wide variety of organs in both species but not found in mouse spleen, in which the expression level was highest in human [our unpublished observation]. Although the name of *NFKBIL1* or IKBL was originally used because of the structural similarity to I kappa B protein, a cytosolic protein which binds to and inhibits NF kappa B, the function of IKBL remains unknown. We tried to but could not demonstrate either augmenting or inhibitory effect on the kappa B enhancer-dependent transcription by overexpression of IKBL protein [unpublished observation]. It was reported that the expression of *NFKBIL1* was rather inversely regulated to that of other members of the I kappa B family [25]. The similarity between IKBL and I kappa B proteins appeared so limited to only a part of ankyrin-like domain which is a well-known motif of protein–protein interaction [26]. Because IKBL protein is localized in the nucleus [27, and our unpublished observation], which is totally different from the cytosolic distribution of I kappa B [28], the function of IKBL may be quite different from that of I kappa B. We are currently in search of the binding molecule(s) of IKBL protein, which may exist in the nucleus, to reveal genuine function(s) of IKBL protein in the cell.

ACKNOWLEDGMENTS

This work was supported in part by Grant-in-Aids from the Ministry of Education, Culture, Sports, Science and Technology and by Grant-in-Aids from the Ministry of Health, Labor, and Welfare in Japan.

REFERENCES

1. Kimura A, Kitamura H, Date Y, Numano F: Comprehensive analysis of HLA genes in Takayasu arteritis in Japan. Int J Cardiol 54:S61, 1996.
2. Kimura A, Ota M, Katsuyama Y, Ohbuchi N, Takahashi M, Kobayashi Y, Inoko H, Numano F: Mapping of the HLA-linked genes controlling the susceptibility to Takayasu's arteritis. Int J Cardiol 75:S105, 2000.
3. Subramanyan R, Joy J, Balakrishnan KG: Natural history of aortoarteritis (Takayasu's disease). Circulation 80:429, 1989.
4. Cid MC, Font C, Coll-Vinent B, Grau JM: Large vessel vasculitides. Curr Opin Rheumatol 10:18, 1998.

5. Gorman JD, Lum RF, Chen JJ, Suarez-Almazor ME, Thomson G, Criswell LA: Impact of shared epitope genotype and ethnicity on erosive disease: a meta-analysis of 3,240 rheumatoid arthritis patients. Arthritis Rheum 50: 400, 2004.
6. Ota M, Katsuyama Y, Kimura A, Tsuchiya K, Kondo M, Naruse T, Itoh K, Sasazuki T, Inoko H: A second susceptibility gene for developing rheumatoid arthritis in the human MHC is localized within a 70-kb interval telomeric of the TNF genes in the HLA class III region. Genomics 71:263, 2001.
7. Albertella MR, Campbell RD: Characterization of a novel gene in the human major histocompatibility complex that encodes a potential new member of the I kappa B family of proteins. Hum Mol Genet 3:793, 1994.
8. Okamoto K, Makino S, Yoshikawa Y, Takaki A, Nagatsuka Y, Ota M, Tamiya G, Kimura A, Bahram S, Inoko H: Identification of I kappa BL as the second major histocompatibility complex-linked susceptibility locus for rheumatoid arthritis. Am J Hum Genet 72:303, 2003.
9. Arguello JR, Little AM, Pay AL, Gallardo D, Rojas I, Marsh SG, Goldman JM, Madrigal JA: Mutation detection and typing of polymorphic loci through double-strand conformation analysis. Nat Genet 18:192, 1998.
10. Kitamura H, Kobayashi Y, Kimura A, Numano F: Association of clinical manifestations with HLA-B alleles in Takayasu arteritis. Int J Cardiol 66:S121, 1998.
11. Tsuchiya K, Kimura A, Kondo M, Nishimura Y, Sasazuki T: Combination of HLA-A and HLA class II alleles controls the susceptibility to rheumatoid arthritis. Tissue Antigens 58:395, 2001.
12. Hoshino S, Kimura A, Fukuda Y, Dohi K, Sasazuki T: Polymerase chain reaction-single-strand conformation polymorphism analysis of polymorphism in DPA1 and DPB1 genes: a simple, economical, and rapid method for histocompatibility testing. Hum Immunol 33:98, 1992.
13. Ho SN, Hunt HD, Horton RM, Pullen JK, Pease LR: Site-directed mutagenesis by overlap extension using the polymerase chain reaction. Gene 77:51, 1989.
14. Bland JM, Altman DG: The odds ratio. Br Med J 320: 1468, 2000.
15. Lewontin RC: The interaction of selection and linkage. I. General considerations; heterotic models. Genetics 49:49, 1964.
16. Hill WG, Robertson A: Linkage disequilibrium in finite populations. Theor Appl Genet 38:226, 1968.
17. Slatkin M, Excoffier L: Testing for linkage disequilibrium in genotypic data using the expectation-maximization algorithm. Heredity 76:377, 1996.
18. Svejgaard A, Ryder LP: HLA and disease associations: detecting the strongest association. Tissue Antigens 43: 18, 1994.
19. Sadowski I, Ma J, Triezenberg S, Ptashne M: GAL4-VP16 is an unusually potent transcriptional activator. Nature 335:563, 1988.
20. Hartley JL, Gregori TJ: Cloning multiple copies of a DNA segment. Gene 13:347, 1981.
21. Yunis EJ, Larsen CE, Fernandez-Vina M, Awdeh ZL, Romero T, Hansen JA, Alper CA: Inheritable variable sizes of DNA stretches in the human MHC: conserved extended haplotypes and their fragments or blocks. Tissue Antigens 62:1, 2003.
22. Yee AS, Raychaudhuri P, Jakoi L, Nevins JR: The adenovirus-inducible factor E2F stimulates transcription after specific DNA binding. Mol Cell Biol 9:578, 1989.
23. Kunsch C, Ruben SM, Rosen CA: Selection of optimal kappa B/Rel DNA-binding motifs: interaction of both subunits of NF-kappa B with DNA is required for transcriptional activation. Mol Cell Biol 12:4412, 1992.
24. Yamashita T, Hamaguchi K, Kusuda Y, Kimura A, Sakata T, Yoshimatsu H: IKBL promoter polymorphism is strongly associated with resistance to type 1 diabetes in Japanese. Tissue Antigens 63:223, 2004.
25. Handel-Fernandez ME, Vincek V: Sequence analysis and expression of a mouse homolog of human IkappaBL gene. Biochim Biophys Acta 1444:306, 1999.
26. Jacobs MD, Harrison SC: Structure of an IkappaBalpha/NF-kappaB complex. Cell 95:749, 1998.
27. Semple JI, Brown SE, Sanderson CM, Campbell RD: A distinct bipartite motif is required for the localization of inhibitory kappaB-like (IkappaBL) protein to nuclear speckles. Biochem J 361:489, 2002.
28. Baeuerle PA, Baltimore D: I kappa B: a specific inhibitor of the NF-kappa B transcription factor. Science 242:540, 1988.
29. Hamaguchi K, Kimura A, Seki N, Higuchi T, Yasunaga S, Takahashi M, Sasazuki T, Kusuda Y, Okeda T, Itoh K, Sakata T: Analysis of tumor necrosis factor-α promoter polymorphism in type 1 diabetes: HLA-B and DRB1 alleles are primarily associated with the disease in Japanese. Tissue Antigens 55:10, 2000.

Apolipoprotein B mRNA–Editing Enzyme, Catalytic Polypeptide–Like 3G: A Possible Role in the Resistance to HIV of HIV-Exposed Seronegative Individuals

Mara Biasin,[1,a] Luca Piacentini,[1,a] Sergio Lo Caputo,[2] Yasuyoshi Kanari,[3] Giuliana Magri,[1] Daria Trabattoni,[1] Valentina Naddeo,[1] Lucia Lopalco,[4] Alberto Clivio,[5] Eugenio Cesana,[5] Francesca Fasano,[1] Cristina Bergamaschi,[1] Francesco Mazzotta,[2] Masaaki Miyazawa,[3] and Mario Clerici[1]

Departments of [1]Immunology and [5]Biology, DISP LITA Vialba, Milano University Medical School, Milano, and [2]Infectious Diseases Clinic, S. M. Annunziata Hospital, Antella, Firenze, Italy; [3]Department of Immunology, Kinki University School of Medicine, Osaka-Sayama, Osaka, Japan; and [4]Duke University Medical Center, Department of Surgery, Laboratory for AIDS Vaccine Research and Development, Durham, North Carolina

Apolipoprotein B mRNA–editing enzyme, catalytic polypeptide–like 3G (APOBEC3G), a human cytidine deaminase, is a potent inhibitor of HIV replication. To explore a possible role of this protein in modulating in vivo susceptibility to HIV infection, we analyzed APOBEC3G expression in HIV-exposed seronegative individuals, HIV-seropositive patients, and healthy control subjects. The results showed that the expression of APOBEC3G is significantly increased in peripheral blood mononuclear cells (PBMCs)—mainly $CD14^+$ cells—and in cervical tissues of HIV-exposed seronegative individuals. Higher APOBEC3G expression correlated with a reduced susceptibility of PBMCs to in vitro infection with the HIV-$1_{Ba\text{-}L}$ R5 strain. APOBEC3G could be important in modulating in vivo susceptibility to sexually transmitted HIV infection.

Apolipoprotein B mRNA–editing enzyme, catalytic polypeptide–like 3G (APOBEC3G) belongs to a family of at least 10 other proteins with broad antiretroviral activity. After the initiation of the reverse transcription of the HIV RNA genome into DNA, the cytidine deaminase activity of APOBEC3G catalyzes the conversion of cytosine to uracil in negative-strand viral cDNA, resulting in the reduction of viral fitness [1, 2]. The viral infectivity factor (Vif) protein of HIV counteracts the activity of APOBEC3G, inducing its degradation by a ubiquitine-proteasome pathway [3].

Susceptibility to HIV is widely different among humans [4, 5]. To verify whether APOBEC3G is involved in modulating susceptibility to HIV infection, we analyzed the expression of this protein in peripheral blood mononuclear cells (PBMCs) and cervical biopsy samples from individuals who, in spite of repeated exposure to HIV, do not become infected (HIV-exposed seronegative individuals). APOBEC3G expression was also evaluated in in vitro HIV infection assays performed on PBMCs from healthy control subjects and HIV-exposed seronegative individuals.

Methods. This study was approved by the institutional review boards of the S. M. Annunziata Hospital; written, informed consent was obtained from all patients. Blood samples were collected from 30 HIV-exposed seronegative individuals. Inclusion criteria were a history of multiple unprotected sexual episodes for ≥4 years at the time of the enrollment, with at least 8 episodes of at-risk intercourse within the 4 months before study entry and an average of 30 (range, 18 to >100) reported unprotected sexual contacts per year. Thirty age-matched HIV-infected patients and 30 age-matched healthy control subjects without any known risk factor for HIV infection were also included in the study. All HIV-seropositive patients were undergoing highly active antiretroviral therapy. All women underwent gynecologic and laboratory evaluation that did not reveal any concomitant infectious or gynecological problems. Cervical biopsy samples from 7 HIV-exposed seronegative individuals, 5 HIV-infected patients, and 7 healthy control subjects were collected in vials containing 1 mL of RNAlater (Ambion). Multiple PBMC samples (mean, 3 samples; range, 2–4 samples) but only 1 cervical biopsy sample was collected from each patient over a period of 3 months, to minimize sampling errors. The final results were expressed as mean values.

For PBMC and $CD4^+$, $CD8^+$, and $CD14^+$ cell isolation and

Received 20 September 2006; accepted 3 November 2006; electronically published XX January 2007.

Reprints or correspondence: Dr. Mario Clerici, Chair of Immunology, University of Milan DISP LITA Vialba, Via G.B. Grassi 74, 20157 Milano, Italy (mario.clerici@unimi.it).

The Journal of Infectious Diseases 2007; 195:000–000

0022-1899/2007/19506-00XX$15.00
DOI: 10.1086/511988

Potential conflicts of interest: none reported.
Presented in part: AIDS 2006, XVI International AIDS Conference, 13–18 August 2006, Toronto, Canada (abstract MOPE0023).
Financial support: Istituto Superiore di Sanità "Programma Nazionale di Ricerca sull' AIDS"; Centro di Eccellenza CISI; EMPRO and AVIP EC WP6 Projects; Japan Health Science Foundation; Tuscany Region, DG Right to Health and Solidarity Policy.
[a] M.B. and L.P. contributed equally to this work.

culture, whole blood was collected by venipuncture in Vacutainer tubes containing EDTA (Becton-Dickinson), and PBMCs were separated on lymphocyte separation medium (Organon Teknica). $CD4^+$ and $CD8^+$ lymphocyte isolation was done with the RosetteSep kit (StemCell Technologies), in accordance with the manufacturer's instructions. $CD8^+$ and $CD4^+$ cell purity was assessed by flow cytometry and ranged between 89% and 97% and between 85% and 94%, respectively. Monocytes were isolated with the Monocyte Isolation Kit (Miltenyi Biotec). Purity (range, 88%–94%) was evaluated by flow cytometry. Cells were cultivated in medium alone (RPMI 1640 and 20% fetal bovine serum [FBS]) or in the presence of 400 U/mL recombinant human interferon (IFN)–α (R&D) for either 4 (mRNA extraction) or 8 (protein extraction) h.

For real-time polymerase chain reaction (PCR), total RNA was extracted from cells or cervical biopsy samples with RNAqueos (Ambion) and were retrotranscribed as described elsewhere [6]. cDNA quantification for APOBEC3G and GAPDH was performed by real-time PCR (DNA Engine Opticon 2; MJ Research). Reactions were performed using a SYBR Green PCR mix (Finnzymes), as described elsewhere [6]. Primer sequences were designed to distinguish among the highly homologous sequences of cytidine deaminases (for APOBEC3G, 5′-CCGTCTGGCTGTGCTACGAA-3′ [forward] and 5′-GCTTCCTCCACTTGCTGAACCA-3′ [reverse]); for GAPDH, 5′-CGGATTTGGTCGTATTGGG-3′ [forward] and 5′-GCTTCCCGTTCTCAGCCTTG-3′ [reverse]). Results were expressed as $\Delta\Delta$Ct (where "Ct" is the cycle threshold) and presented as ratios between the target gene and the GAPDH housekeeping mRNA.

For quantification of APOBEC3G protein by ELISA, total proteins extracted with an M-Per reagent and Halt Protease Inhibitor Cocktail (Pierce) were quantified by a BCA assay (Pierce). Ten micrograms of sample was coated on a 96-well plate overnight at 4°C. After blocking with 5% bovine serum albumin in Tris-buffered saline, the samples were incubated with 5 μg/mL chicken anti-APOBEC3G antibody, produced and characterized in our laboratory (Clivio A. et al; manuscript in preparation), for 2 h at 37°C. After a wash step, an anti-IgY–horseradish peroxidase conjugate (diluted 1:8000; Promega) was added. The coloring reaction was performed with the TMB Microwell Peroxidase Substrate (KPL).

For IFN-α receptor 1 (IFNAR1) analysis, PBMCs were stained for 1 h at 4°C in the dark with an anti–human IFN-α/β receptor 1 biotinylated antibody (R&D Systems), anti-CD4–phycoerythrin (PE), and CD8-PE-Cy5 or with biotinylated anti-human IFN-α/B receptor 1 and anti-CD14–PE–Cy5 (Caltag Laboratories). Cytometric analysis was performed using an FC500 flow cytometer (Beckman Coulter).

For the in vitro challenge assay, PBMCs (2×10^6 cells/mL) were cultured for 2 days at 37°C and 5% CO_2 in RPMI 1640 containing FBS (20%), phytohemagglutinin (5 μg/mL), and interleukin (IL)–2 (10 ng/mL). After viability assessment and $CD4^+$ and $CD8^+$ cell percentage evaluation, done as described elsewhere [7], 3×10^6 cells were resuspended in medium containing 0.05 ng of HIV-$1_{Ba\text{-}L}$ p24 viral input and incubated for 3 h at 37°C. Cells were then washed and resuspended in 3 mL of complete medium with IL-2 (10 ng/mL). Cells were plated in 24-well tissue culture plates and incubated at 37°C and 5% CO_2. PBMCs were then divided into 3 wells to be analyzed on days 2, 3, and 5. Cultures were refed with complete medium plus IL-2 on day 3, and supernatants were collected for batched ELISA of p24 antigen. Absolute levels of p24 were measured using the Alliance HIV-1 p24 ELISA Kit (PerkinElmer), and APOBEC3G protein expression was evaluated by ELISA.

Statistical analyses were performed using SPSS (SPSS). Differences between the groups were assessed using nonparametric analyses (Mann-Whitney U test). The standard t test was used for comparing different conditions within the same group. All P values are two-tailed.

Results. APOBEC3G mRNA expression in unstimulated PBMCs was significantly augmented in HIV-exposed seronegative individuals, compared with that in healthy control subjects ($P = .042$). IFN-α stimulation resulted in a 3-fold increase in APOBEC3G mRNA levels in PBMCs from HIV-exposed seronegative individuals ($P = .001$) but had only a modest effect in HIV-infected patients and healthy control subjects. As a result, APOBEC3G mRNA levels in IFN-α–stimulated PBMCs were significantly augmented in HIV-exposed seronegative individuals, compared with those in both healthy control subjects ($P = .042$) and HIV-infected patients ($P = .026$) (figure 1*A*).

ELISA results confirmed that the highest levels of APOBEC3G protein were detected in PBMCs from HIV-exposed seronegative individuals, both in basal conditions ($P = .006$, vs. HIV-infected patients) and after IFN-α stimulation ($P = .001$, vs. HIV-infected patients; $P = .031$, vs. healthy control subjects) (figure 1*B*).

IFN-α stimulation of $CD14^+$ cells resulted in a 20-, 9-, and 6-fold increase in APOBEC3G mRNA levels in HIV-exposed seronegative individuals, healthy control subjects, and HIV-infected patients, respectively ($P = .42$, for HIV-exposed seronegative individuals vs. healthy control subjects) (figure 1*C*). A weaker effect was seen for $CD4^+$ cells (6-, 4-, and 3-fold increase in HIV-exposed seronegative individuals, HIV-infected patients, and healthy control subjects, respectively), whereas IFN-α–induced modulation of APOBEC3G mRNA levels was minimal (<2-fold increase) in $CD8^+$ cells from all individuals included in the study (figure 1*C*). ELISA analyses of APOBEC3G protein in $CD14^+$ cells confirmed these results by showing higher levels of APOBEC3G in $CD14^+$ cells from HIV-exposed seronegative individuals than in healthy control subjects and HIV-infected patients, both in basal condition and after IFN-α stimulation (figure 1*D*).

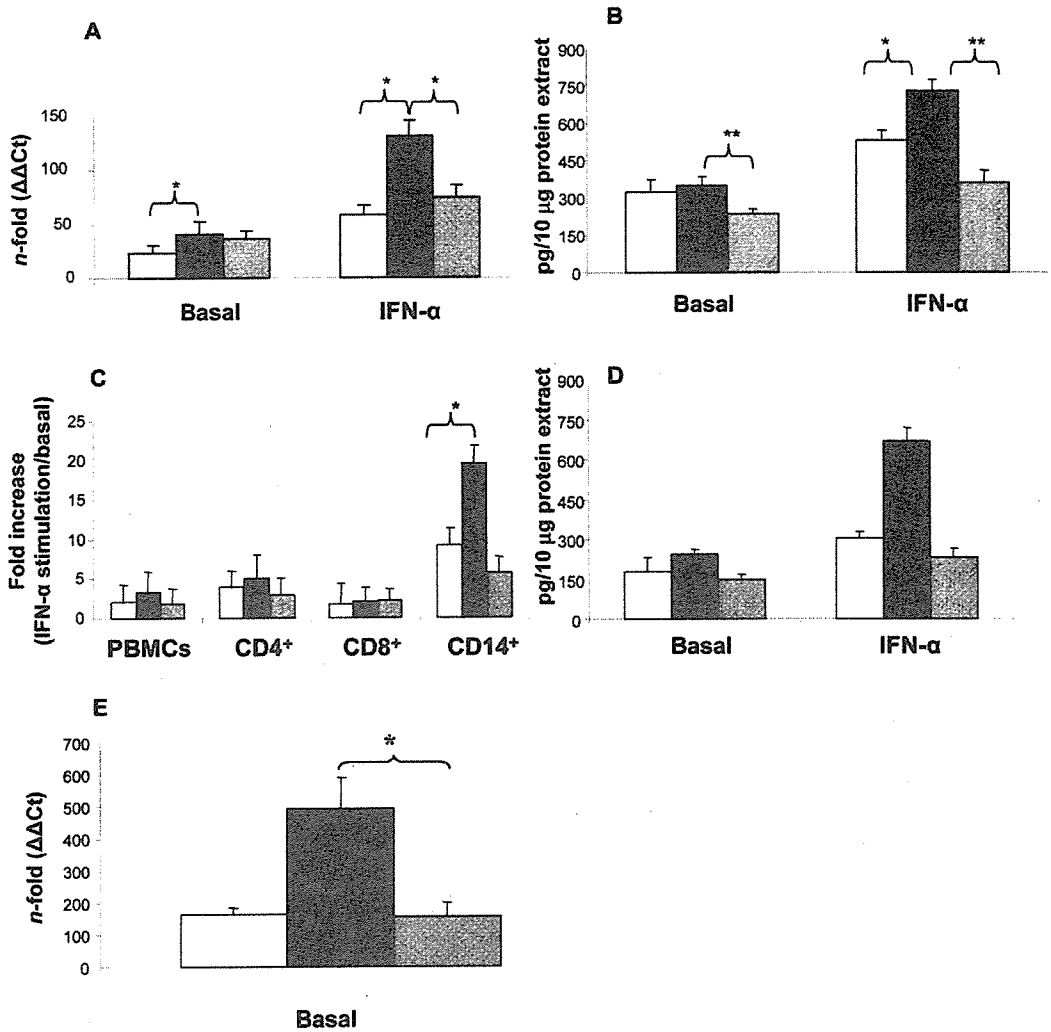

Figure 1. *A*, Apolipoprotein B mRNA–editing enzyme, catalytic polypeptide–like 3G (APOBEC3G) mRNA expression in basal conditions and after stimulation with 400 U/mL interferon (IFN)–α in peripheral blood mononuclear cells (PBMCs) from healthy control subjects *(white bars)*, HIV-exposed seronegative individuals *(black bars)*, and HIV-infected patients *(grey bars)*. *B*, APOBEC3G protein quantification by ELISA in PBMCs from healthy control subjects *(white bars)*, HIV-exposed seronegative individuals *(black bars)*, and HIV-infected patients *(grey bars)* in basal conditions and after IFN-α stimulation. *C*, Changes in APOBEC3G mRNA expression after IFN-α stimulation of PBMCs and CD4+, CD8+, and CD14+ cells isolated from healthy control subjects *(white bars)*, HIV-exposed seronegative individuals *(black bars)*, and HIV-infected patients *(grey bars)*. *D*, APOBEC3G protein quantification by ELISA in CD14+ cells from healthy control subjects *(white bars)*, HIV-exposed seronegative individuals *(black bars)*, and HIV-infected patients *(grey bars)* in basal conditions and after IFN-α stimulation. *E*, APOBEC3G mRNA expression in cervical biopsy samples from healthy control subjects *(white bars)*, HIV-exposed seronegative individuals *(black bars)*, and HIV-infected patients *(grey bars)*. Results are mean ± SE values. Ct, cycle threshold. **P* < .05; ***P* < .01

Flow cytometry analysis (mean fluorescence intensity) showed that IFNAR1 expression was significantly higher in CD14+ cells (mean ± SE percentage of IFNAR1-positive cells, 8.2% ± 3.8% for HIV-exposed seronegative individuals, 7.9% ± 3.6% for HIV-infected patients, and 8.3% ± 3.1% for healthy control subjects) than in both CD4+ cells (2.9% ± 0.6% for HIV-exposed seronegative individuals, 3.5% ± 1.3% for HIV-infected patients, and 3.0% ± 1.4% for healthy control subjects) and CD8+ cells (3.7% ± 1.1% for HIV-exposed seronegative individuals, 4.5% ± 2.6% for HIV-infected patients, and 4.2% ± 1.9% for healthy control subjects), providing a possible explanation for the enhanced responsiveness of monocytes to IFN-α. Surface levels of IFNAR1 on CD14+ cells were, nevertheless, comparable among the 3 groups of individuals.

APOBEC3G mRNA levels were significantly increased in cervical biopsy samples from HIV-exposed seronegative individuals, compared with those in HIV-infected patients and healthy control subjects ($P = .024$, vs. HIV-infected patients) (figure 1*E*). Unfortunately, protein analyses could not be performed because of a limitation in the amount of available material.

In vitro HIV infection of PBMCs from HIV-exposed seronegative individuals resulted in a lower amount of p24 after 2,

3, and 5 days, compared with that in PBMCs from healthy control subjects. This result was not likely to be due to quantitative differences in $CD4^+$ and $CD8^+$ cells, because the median $CD4^+$ (45% ± 6% for HIV-exposed seronegative individuals and 44% ± 5% for healthy control subjects) and $CD8^+$ (20% ± 3% for HIV-exposed seronegative individuals and 19% ± 4% for healthy control subjects) T cell percentage was comparable between the 2 groups. Quantification of APOBEC3G protein by ELISA showed that PBMCs from HIV-exposed seronegative individuals produced higher levels of APOBEC3G on days 2, 3, and 5 than did those from healthy control subjects. Differences were statistically significant ($P < .05$) at day 5 (table 1).

Discussion. In this study, we investigated whether the reduced susceptibility to HIV infection that characterizes HIV-exposed seronegative individuals could be related to differential expression of APOBEC3G and whether the expression of this protein could be differently modulated by exposure to IFN-α. The results showed that APOBEC3G mRNA levels were significantly increased in PBMCs from both HIV-exposed seronegative individuals and HIV-infected patients, compared with those in PBMCs from healthy control subjects. In contrast, levels of APOBEC3G protein were significantly augmented only in PBMCs from HIV-exposed seronegative individuals. The chronic exposure to HIV taking place in HIV-infected patients and HIV-exposed seronegative individuals could explain why APOBEC3G mRNA expression is stimulated in both. The Vif protein of HIV induces the degradation of APOBEC3G by a ubiquitine-proteasome pathway. By definition, HIV infection does not take place in HIV-exposed seronegative individuals [8]: in these individuals, the absence of Vif would prevent APOBEC3G degradation, possibly justifying the discrepancy between mRNA and protein levels.

After IFN-α stimulation, both APOBEC3G mRNA and protein levels increased in the 3 groups studied, with a more pronounced effect in HIV-exposed seronegative individuals than in both HIV-infected patients and healthy control subjects. Although IFN-α–induced modulation of APOBEC3G levels could seem relatively modest (3-fold), it has been demonstrated that even slight changes in the in vitro expression of APOBEC3G result in the reduction of HIV infectivity. These results, thus, suggest that population-level variation in APOBEC3G and Vif levels are likely to deeply influence the outcome of infection with HIV [9]. To verify this hypothesis, we performed in vitro infection assays on PBMCs from HIV-exposed seronegative individuals and healthy control subjects. We decided to use a macrophagotropic HIV-1 strain (R5) to approach the situation seen in in vivo primary HIV infection during sexual transmission [10]. Interestingly, the kinetics of changes in p24 and APOBEC3G levels were different in the 2 groups examined. Thus, compared with what was observed in healthy control subjects, in vitro HIV infection of PBMCs from HIV-exposed seronegative individuals resulted in a slower increase in p24 concentration and a much more rapid up-regulation of APOBEC3G. A working hypothesis stemming from these data is that, once exposed to the virus, exposed seronegative individuals would respond to IFN-α production with a faster and more robust increase in the expression of APOBEC3G and a consequent reduced susceptibility to HIV infection.

The present data show that monocytes are exquisitely responsive to IFN-α–induced up-regulation of APOBEC3G. Monocyte-derived type I IFNs are responsible for the earliest phase of the immune responses against pathogens, and their synthesis is directly triggered by viruses [11]. The higher amounts of APOBEC3G proteins seen in IFN-α–stimulated monocytes from HIV-exposed seronegative individuals could result in an amplification of these early, innate defensive immune mechanisms. Presumably, the peculiar responsiveness to IFN-α and up-regulation of APOBEC3G in $CD14^+$ cells observed in HIV-exposed seronegative individuals would be seen not only in monocytes but, more generally, in nonlymphoid cells such as macrophages and Langerhans cells. It is tempting to speculate that the higher quantity of APOBEC3G produced by monocyte-derived cells, including Langerhans cells and macrophages, that cluster in peripheral tissues at mucosal sites could constitute an important barrier to HIV penetration during sexual exposure. This hypothesis is reinforced by the observation that APOBEC3G mRNA expression was indeed increased in cervical biopsy samples from HIV-exposed seronegative individuals.

Recent findings have demonstrated that APOBEC3G can ex-

Table 1. p24 concentration in supernatants and apolipoprotein B mRNA–editing enzyme, catalytic polypeptide–like 3G (APOBEC3G) protein expression level in peripheral blood mononuclear cells from HIV-exposed seronegative individuals and healthy control subjects.

Day, protein	Exposed/seronegative (n = 10)	Healthy controls (n = 10)
Day 2		
p24, pg/mL	4 ± 0.8	21 ± 7.2
APOBEC3G, HIV challenge/basal	1.43 ± 0.15	0.98 ± 0.23
Day 3		
p24, pg/mL	96 ± 23.0	357 ± 79.5
APOBEC3G, HIV challenge/basal	2.91 ± 0.63	1.17 ± 0.32
Day 5		
p24, pg/mL	4315 ± 114.3	16613 ± 175.6
APOBEC3G, HIV challenge/basal	4.01 ± 0.54[a]	2.03 ± 0.85

NOTE. Data are mean ± SE values. Cultures were infected with limiting amounts (0.05 ng of p24 viral input) of the HIV-1_{Ba-L} R5 strain.

[a] $P < .05$.

ist into 2 different forms: an active one (low molecular weight [LMW]) and an inactive one (high molecular weight [HMW]) [12, 13]. It will be interesting to evaluate whether the prevalent localization of APOBEC3G in LMW and HMW complexes differs in HIV-exposed seronegative individuals. Similarly, we will q19 evaluate in our cohort the presence of the C40693T *APOBEC3G* gene sequence variant recently associated with an increased risk of infection [14].

Given that, worldwide, the vast majority of HIV infections are sexually acquired [15], a potent APOBEC3G-mediated systemic and mucosal antiviral response could offer a formidable barrier against HIV infection. The present results could play q20 an important role in the design of new therapeutic and vaccine strategies.

References

1. Zhang H, Yang B, Pomerantz RJ, Zhang C, Arunachalam SC, Gao L. The cytidine deaminase CEM15 induces hypermutation in newly synthesized HIV-1 DNA. Nature **2003**; 424:94–8.
2. Mangeat B, Turelli P, Caron G, Friedli M, Perrin L, Trono D. Broad antiretroviral defence by human APOBEC3G through lethal editing of nascent reverse transcripts. Nature **2003**; 424:99–103.
3. Yu X, Yu Y, Liu B, et al. Induction of APOBEC3G ubiquitination and degradation by an HIV-1 Vif-Cul5-SCF complex. Science **2003**; 302: 1056–60.
4. Rowland-Jones SL, McMichael A. Immune responses in HIV-exposed-seronegatives: have they repelled the virus? Curr Opin Immunol **1995**;7: 448–53.
5. Shearer GM, Clerici M. Protective immunity against HIV infection: has nature done the experiment for us? Immunol Today **1996**; 17:21–6.
6. Milazzo L, Biasin M, Gatti N, et al. Thalidomide in the treatment of chronic hepatitis C unresponsive to alfa-interferon and ribavirin. Am J Gastroenterol **2006**; 101:399–402.
7. Schenal M, Lo Caputo S, Fasano F, et al. Distinct patterns of HIV-specific memory T lymphocytes in HIV-exposed uninfected individuals and in HIV-infected patients. AIDS **2005**; 19:653–61.
8. Biasin M, Caputo SL, Speciale L, et al. Mucosal and systemic immune activation is present in human immunodeficiency virus–exposed seronegative women. J Infect Dis **2000**; 182:1365–74.
9. Mariani R, Chen D, Schrofelbauer B, et al. Species-specific exclusion of APOBEC3G from HIV-1 virions by Vif. Cell **2003**; 114:21–31.
10. Berlier W, Bourlet T, Lawrence P, et al. Selective sequestration of X4 isolates by human genital epithelial cells: implication for virus tropism selection process during sexual transmission of HIV. J Med Virol **2005**; 77:465–74.
11. Friedman RM. Interferons. In: Oppenheim JJ, Shevach EM, eds. Textbook of immunophysiology. New York: Oxford University Press, **1988**: 94–144.
12. Chiu YL, Soros VB, Kreisberg JF, Stopak K, Yonemoto W, Green WC. q21 Cellular APOBEC3G restricts HIV-1 infection in resting CD4+ T cells. Nature **2005**; 435:108–14.
13. Chen K, Huang J, Zhang C, et al. Alpha interferon potently enhances the anti-human immunodeficiency virus type 1 activity of APOBEC3G in resting primary CD4 T cells. J Virol **2006**; 80:7645–57.
14. Valcke HS, Bernard NF, Bruneau J, Alary M, Tsoukas CM, Roger M. APOBEC3G genetic variants and their association with risk of HIV infection in highly exposed Caucasians. AIDS **2006**; 20:1984–6.
15. Quinn TC. Global burden of the HIV-1 pandemic. Lancet **1996**; 348: 99–106.

MHC Class I-Like MILL Molecules Are β_2-Microglobulin-Associated, GPI-Anchored Glycoproteins That Do Not Require TAP for Cell Surface Expression[1]

Mizuho Kajikawa,*† Tomohisa Baba,‡ Utano Tomaru,‡ Yutaka Watanabe,* Satoru Koganei,§ Sachiyo Tsuji-Kawahara,¶ Naoki Matsumoto,§ Kazuo Yamamoto,§ Masaaki Miyazawa,¶ Katsumi Maenaka,† Akihiro Ishizu,‡‖ and Masanori Kasahara[2]*‡

MILL (MHC class I-like located near the leukocyte receptor complex) is a family of MHC class I-like molecules encoded outside the MHC, which displays the highest sequence similarity to human MICA/B molecules among known class I molecules. In the present study, we show that the two members of the mouse MILL family, MILL1 and MILL2, are GPI-anchored glycoproteins associated with β_2-microglobulin (β_2m) and that cell surface expression of MILL1 or MILL2 does not require functional TAP molecules. MILL1 and MILL2 molecules expressed in bacteria could be refolded in the presence of β_2m, without adding any peptides. Hence, neither MILL1 nor MILL2 is likely to be involved in the presentation of peptides. Immunohistochemical analysis revealed that MILL1 is expressed in a subpopulation of thymic medullary epithelial cells and a restricted region of inner root sheaths in hair follicles. The present study provides additional evidence that MILL is a class I family distinct from MICA/B. *The Journal of Immunology*, **2006, 177: 3108–3115.**

Classical MHC class I molecules, also known as class Ia, are heterodimeric glycoproteins made up of a transmembrane-type H chain and β_2-microglobulin (β_2m).[3] They bind small peptides primarily derived from cytosolic proteins in a groove comprised of the α1 and α2 domains and present them to $CD8^+$ T cells, thereby enabling the immune system to destroy abnormal cells that synthesize viral or other foreign proteins (1). Class Ia molecules are almost ubiquitously expressed and their H chains exhibit an extraordinary level of polymorphism (2).

By contrast, class I molecules, collectively called nonclassical class I or class Ib, are usually oligomorphic or monomorphic, and do not necessarily bind peptides (3–5). Many class Ib molecules have a more restricted tissue distribution than class Ia molecules. Although the majority of class Ib molecules form complexes with β_2m, MICA/B (MHC class I-related chains A and B) (6), zinc-α2-glycoprotein (7), the endothelial protein C receptor (8), and the RAE-1 (retinoic acid early inducible-1) family of class Ib molecules (9) are not associated with β_2m. Furthermore, a significant proportion of class Ib genes (the genes coding for the H chains of class Ib molecules) are located outside the MHC region (5). Accumulated evidence indicates that class Ib molecules have diverse functions ranging from specialized Ag presentation (10–12) to the activation of NK cells (13, 14), transport of IgG (15), pheromone detection (16, 17), and lipid mobilization and catabolism (18).

Recently, we identified a new family of class Ib genes designated *Mill* (MHC class I-like located near the leukocyte receptor complex) in mice (19) and rats (20). The two members of the *Mill* family, *Mill1* and *Mill2*, are located close to the leukocyte receptor complex, thus outside the MHC. *Mill1* and *Mill2* show only limited levels of polymorphism and are transcribed at low levels in most adult tissues. RT-PCR analysis showed that *Mill1* is transcribed in selected tissues such as neonatal thymus and skin whereas *Mill2* is transcribed more ubiquitously at low levels. Predicted MILL1 and MILL2 molecules are glycoproteins with three extracellular domains (α1 to α3), but their α1 and α2 domains lack many of the residues essential for the docking of peptides, suggesting that MILL molecules do not bind peptides. Phylogenetically, MILL1 and MILL2 are most closely related to MICA/B among known class I molecules. Because rodents lack the MICA/B family and conversely, humans do not have the MILL family, we suggested previously that MILL might be a functional substitute for MICA/B (19).

In the present study, we show that MILL1 and MILL2 are GPI-anchored glycoproteins associated with β_2m. Consistent with the absence of critical residues required for the docking of peptides (19), cell surface expression of MILL1 and MILL2 did not require TAP molecules. Immunohistochemical analysis revealed that MILL1 is expressed in a subpopulation of thymic medullary epithelial cells and a restricted region of inner root sheaths in hair follicles. The ability to form complexes with β_2m, anchorage to the membrane by GPI, and unique expression patterns all provide further evidence that MILL is a class I family distinct from MICA/B.

*Department of Biosystems Science, School of Advanced Sciences, Graduate University for Advanced Studies (Sokendai), Hayama, Japan; †Division of Structural Biology, Medical Institute of Bioregulation, Kyushu University, Fukuoka, Japan; ‡Department of Pathology, Hokkaido University Graduate School of Medicine, Sapporo, Japan; §Department of Integrated Biosciences, Graduate School of Frontier Sciences, University of Tokyo, Chiba, Japan; ¶Department of Immunology, Kinki University School of Medicine, Osaka, Japan; and ‖Department of Medical Technology, Hokkaido University School of Medicine, Sapporo, Japan

Received for publication July 26, 2005. Accepted for publication June 16, 2006.

The costs of publication of this article were defrayed in part by the payment of page charges. This article must therefore be hereby marked *advertisement* in accordance with 18 U.S.C. Section 1734 solely to indicate this fact.

[1] This work was supported by grants-in-aid for Scientific Research from the Ministry of Education, Culture, Sports, Science and Technology of Japan, Uehara Memorial Foundation, the Naito Foundation, and the Takeda Science Foundation.

[2] Address correspondence and reprint requests to Dr. Masanori Kasahara, Department of Pathology, Hokkaido University Graduate School of Medicine, North-15, West-7, Sapporo 060-8638, Japan. E-mail address: mkasaha@med.hokudai.ac.jp

[3] Abbreviations used in this paper: β_2m, β_2-microglobulin; MILL, MHC class I-like located near the leukocyte receptor complex; PI-PLC, phosphatidylinositol-specific phospholipase C; PNGase F, peptide:*N*-glycosidase F.

0022-1767/06/$02.00

Materials and Methods

Cell lines and Abs

The mouse T lymphoma cell line RMA ($H2^b$-positive) and its TAP2-deficient mutant RMA-S ($H2^b$-negative) (21) were obtained from Dr. Kärre (Karolinska Institute, Stockholm, Sweden). Cells were maintained in RPMI 1640 medium (Invitrogen) supplemented with 10% (v/v) heat-inactivated FBS at 37°C and 5% CO_2.

Anti-FLAG mAb M2 (F3165) was purchased from Sigma-Aldrich. Goat polyclonal Ab to mouse β_2m (sc-8361) was purchased from Santa Cruz Biotechnology. Anti-human pan-cytokeratin mAb AE1/AE3 (M1590) and anti-human hair shaft cytokeratin mAb AE13 (ab16113) were purchased from DakoCytomation and Abcam, respectively. Mouse anti-H2-K^b mAb (clone AF6–88.5) and anti-CD45 mAb (clone 30-F11) were from BD Pharmingen. The Abs used as secondary reagents were as follows: FITC-labeled goat anti-mouse IgG, $F(ab')_2$ fragment (IM0819; Beckman Coulter), FITC-labeled swine anti-rabbit Ig, $F(ab')_2$ fragment (F0054; DakoCytomation), HRP-conjugated sheep anti-mouse IgG (NA931; Amersham Biosciences), HRP-conjugated donkey anti-rabbit IgG (NA934; Amersham Biosciences), HRP-conjugated donkey anti-goat IgG (sc-2056; Santa Cruz Biotechnology), Alexa Fluor 594-conjugated goat anti-rabbit IgG (A11072; Molecular Probes), and Alexa Fluor 488-conjugated goat anti-mouse IgG (A11001; Molecular Probes). Isotype-matched mouse IgG1 Ab (PP100) and pooled normal rabbit serum (CL1000) were purchased from Chemicon International Inc. and Cedarlane Laboratory Ltd., respectively.

Production of polyclonal Ab against mouse MILL molecules

The α1-α3 domains of MILL1 and MILL2 with 6 × His tags at their N termini were expressed in *Escherichia coli* strain M15 using the pQE30 expression vector following the instructions of the manufacturer (Qiagen). Briefly, the DNA fragments encoding the α1-α3 domains of mouse MILL molecules were amplified by PCR using the BALB/c-derived *Mill* plasmid cDNA (19) as templates. The primer sequences were 5′-TTGCGAGCTC CACACTCTGCGCTATGACCT-3′ (with a *Sac*I site at its 5′-end) and 5′-CCCAAGCTTATATTGTGGTTGCCGTGCTT-3′ (with a *Hin*dIII site at its 5′-end) for MILL1 and 5′-GTGGATCCACCCACACTCTGCGC TATAA-3′ (with a *Bam*HI site at its 5′-end) and 5′-CCCAAGCTTCATC CTGACTGTCCTCAGCA-3′ (with a *Hin*dIII site at its 5′-end) for MILL2. PCR products digested with *Sac*I/*Hin*dIII for MILL1 and *Bam*HI/*Hin*dIII for MILL2 were ligated into *Sac*I/*Hin*dIII- and *Bam*HI/*Hin*dIII-digested pQE30, respectively. After transformation into M15, recombinant proteins were induced by adding isopropyl-1-thio-β-D-galactopyranoside to a final concentration of 1 mM. *E. coli* cells were harvested and lysed in buffer B (100 mM NaH_2PO_4, 10 mM Tris-HCl, 6 M guanidine hydrochloride, pH 8.0), and lysates were centrifuged at 10,000 × *g* for 20 min at room temperature. Ni-NTA acid resins were added to supernatants and mixed gently by shaking. Resin-lysate mixtures were loaded into an empty column and washed twice with buffer C (100 mM NaH_2PO_4, 10 mM Tris-HCl, 6 M guanidine hydrochloride, pH 5.9). Recombinant proteins were eluted by buffer D (100 mM NaH_2PO_4, 10 mM Tris-HCl, 6 M guanidine hydrochloride, pH 4.5), separated by preparative SDS-PAGE, eluted and concentrated. Purified recombinant proteins (200 μg per rabbit) were mixed with CFA and injected into rabbits. After 2, 4, and 6 wk, the animals were boosted with the same amount of recombinant proteins mixed with IFA. Whole bloods were collected and antisera prepared 1 wk after the last boost.

Construction of mammalian expression plasmids

Mouse MILL molecules have an insertion of amino acids between the leader peptide and the α1 domain (19). The coding regions of mouse MILL1 and MILL2 excluding this inserted sequence and the leader peptide were obtained by PCR using the *Mill* plasmid cDNA (19) as templates. The primer sequences were 5′-CCAAGCTTGAACCCCACACTCTGCGC TA-3′ (with a *Hin*dIII site at its 5′-end) and 5′-GTGGATCCCTACCAA CACTGTAGAAAAGAGC-3′ (with a *Bam*HI site at its 5′-end) for MILL1 and 5′-CCAAGCTTACCCACACTCTGCGCTATAA-3′ (with a *Hin*dIII site at its 5′-end) and 5′-GTGGATCCTCAGTTGGCTCTGGCCAGTG-3′ (with a *Bam*HI site at its 5′-end) for MILL2. After digestion with *Hin*dIII/*Bam*HI, the PCR products were ligated to the *Hin*dIII/*Bam*HI-digested pFLAG-CMV-3 expression vector carrying a preprotrypsin leader sequence (Sigma-Aldrich). These constructs, designated MILL1-pFLAG-CMV-3 and MILL2-pFLAG-CMV-3, respectively, enabled the expression of MILL molecules with an N-terminal FLAG tag. In all cases, the integrity of expression constructs was verified by sequencing. DNA for transfection was isolated with the plasmid purification kit purchased from Qiagen.

Establishment of stable transfectants

To establish stable cell lines expressing MILL molecules, RMA and RMA-S cells were transfected with linearized MILL1-pFLAG-CMV-3 or MILL2-pFLAG-CMV-3 plasmids by electroporation at 250 V, 950 μF with Gene Pulser II according to the instructions of the manufacturer (Bio-Rad). Neomycin-resistant cells were selected by treatment with G418 (600 and 800 μg/ml for RMA and RMA-S, respectively) and clones exhibiting high levels of MILL expression were expanded; expression of MILL proteins was monitored by flow cytometry and immunoblotting with anti-FLAG and anti-MILL Abs.

Flow cytometric analysis

For cell surface staining, single cell suspensions (1×10^6 cells) were washed with ice-cold PBS (pH 7.4) and incubated in 100 μl of PBS (pH 7.4) containing 0.1% NaN_3 with 1 μg of mAb or isotype controls for 30 min on ice. After washing with ice-cold PBS (pH 7.4), cells were incubated in 100 μl of PBS (pH 7.4) containing 0.1% NaN_3 with the FITC-conjugated $F(ab')$ fragment of goat anti-mouse IgG or $F(ab')_2$ fragment of swine anti-rabbit Ig (1:200 dilution). Subsequently, cells were washed with ice-cold PBS (pH 7.4) and analyzed by EPICS ALTRA (Beckman Coulter). Data were analyzed with EXPO32 software (Beckman Coulter).

Immunoprecipitation and glycosidase digestion

For purification of FLAG-tagged MILL proteins, RMA-MILL1 and RMA-MILL2 stable transfectants (1×10^8 cells) were solubilized by 1 ml of ice-cold lysis buffer (50 mM Tris-HCl, 1 mM EDTA, 150 mM NaCl, 1% Triton X-100, 0.2 mM 4-(2-aminoethyl)-benzenesulfonyl fluoride, 20 μM leupeptin, 1 μM pepstatin, pH 7.5). After incubation for 30 min at 4°C, cell lysates were centrifuged at 13,000 × *g* for 10 min at 4°C to remove cell nuclei and insoluble proteins. Cleared lysates were incubated with protein G-Sepharose beads (Amersham Biosciences) at 4°C for 1 h. Supernatants were incubated with anti-FLAG mAb-coupled protein G-Sepharose beads at 4°C for 1 h. After washing 4 times with lysis buffer, immunoprecipitated proteins were eluted by 0.1 M glycine-HCl (pH 3.0), and immediately neutralized by adding 0.1 M Tris-HCl (pH 9.0). Eluted proteins were denatured and treated with 500 U/μl peptide:*N*-glycosidase F (PNGase F; New England Biolabs) at 37°C for 18 h.

Immunoblotting

To detect MILL proteins and β_2m, samples were incubated in 1 × SDS sample buffer at 95°C for 10 min. Denatured proteins were separated on 12% SDS-PAGE and transferred to Hybond-P polyvinylidene difluoride membranes (Amersham Biosciences) using a semidry blotter (Bio-Rad) at 15 V for 45 min. The blotted membranes were incubated with 5% skim milk or 3% BSA in PBS (pH 7.4) containing 0.1% Tween 20 (PBST) at room temperature for 60 min and then incubated with 1/500 diluted antisera or 1 μg/ml of Ab in PBST at room temperature for 60 min. After washing twice with PBST, the membranes were incubated with 1/25,000 diluted HRP-conjugated anti-mouse, rabbit or goat IgG Abs. After washing three times with PBST, positive bands were visualized using the ECL-Plus (Amersham Biosciences) or the Super Signal West Dura detection system (Pierce).

Phosphatidylinositol-specific phospholipase C (PI-PLC) treatment

RMA-MILL and RMA-S-MILL cells were washed with PBS (pH 7.4) and treated with 1 U/ml PI-PLC (Sigma-Aldrich) in PBS (pH 7.4) at 37°C for 1 h. Subsequently, cells were washed with ice-cold PBS (pH 7.4) and used for flow cytometric analysis.

Coimmunoprecipitation of cell surface MILL molecules

Cell surface MILL proteins expressed on the RMA-MILL stable transfectants were purified by PI-PLC treatment and immunoprecipitation with anti-FLAG Ab-coupled protein G-Sepharose beads. Immunoprecipitates were subjected to immunoblotting using anti-FLAG and anti-mouse β_2m Ab.

Refolding of bacterially expressed MILL ectodomains

cDNA encoding the ectodomains of MILL1 and MILL2 were amplified by PCR using the *Mill* plasmid cDNA (19) as templates. Primers used were 5′-CATTAATGGACAACCAAAGACTGGTG-3′ (sense) and 5′-TCC CCCGGGGGCAGCAGGTTCATTGATA-3′ (antisense) for MILL1, and 5′-CCATATGTCCAGCATCCAAGGAACC-3′ (sense) and 5′-AAAAG TACTGACAGCTGTCTGCATGATG-3′ (antisense) for MILL2. These

primers contained *Ase*I, *Sma*I, *Nde*I, or *Sca*I restriction enzyme sites indicated by underlines. The PCR-generated cDNA fragments of MILL1 and MILL2 were cloned into the bacterial expression vector pET3cN-bio, which was designed to express a recombinant protein with an N-terminal enzymatic biotinylation signal (22), to construct MILL1-pET3cNbio and MILL2-pET3cNbio, respectively. Rosetta (DE3) strain of *E. coli* (Novagen, Merck) was transformed with MILL1-pET3cNbio or MILL2-pET3cNbio. Expression of soluble MILL1 or MILL2 was induced with 1 mM isopropyl-1-thio-β-D-galactopyranoside, and MILL proteins were refolded from the purified inclusion bodies by dilution as described previously (22). To examine effects of β_2m on refolding, C57BL/6-derived β_2m (β_2m^b), similarly expressed in *E. coli*, was included in the refolding mixture at the molar ratio of 1:2 (MILL/β_2m). Refolded soluble MILL1 and MILL2 proteins were purified by anion-exchange column chromatography and gel-filtration chromatography. In anion-exchange chromatography on a UNO Q-6 column using 20 mM Tris-HCl buffer (pH 8.5) as a mobile phase, soluble MILL1 or MILL2 refolded in the presence of β_2m was eluted in the approximately 250 mM Cl^- fraction by a 0–500 mM NaCl gradient. The gel-filtration column chromatography was performed on a Superdex 75 10/30 column (Amersham Biosciences) equilibrated with 25 mM Tris-HCl buffer (pH 8.0) containing 150 mM NaCl at the flow rate of 0.5 ml/min. The column was calibrated with gel-filtration standards from Bio-Rad.

Immunohistochemistry

For immunostaining, frozen sections prepared from 3-day-old, 10-day-old, and 6-wk-old male BALB/c mice were fixed using cold acetone for 5 min, washed with PBS, stained by the standard method (23), and then mounted in fluorescent mounting medium (DakoCytomation). Immunofluorescence was detected using a fluorescence microscope (ECLIPSE E600; Nikon). To evaluate the specificity of staining, the antiserum against MILL1 was diluted 1/40 with PBS to a final volume of 1 ml and absorbed with 5×10^7 RMA-MILL1 or RMA cells at 4°C overnight. The preabsorbed antiserum was diluted 1/80 with PBS and used for immunostaining. All experiments using animals have been reviewed and approved by the institutional review committee of Hokkaido University Graduate School of Medicine.

Isolation of thymic stromal cells

Thymi were dissected from 4-wk-old C57BL/6 and β_2m-deficient mice. Breeding pairs of the β_2m-deficient strain, B6.129P2-*B2m*^{tm1Unc}/J (stock no. 002087), were purchased from The Jackson Laboratory, and their progenies were produced at Kinki University School of Medicine. Thymic stromal cells were enriched as described (24). Briefly, thymic fragments were digested in RPMI 1640 medium containing collagenase D and DNase I (both obtained from Roche) at 37°C for 15 min. After repeating this procedure 3 times, cells were pooled and stained with mAb for CD45. CD45-negative fractions containing stromal cells including thymic epithelial cells were subjected to flow cytometric analysis.

Results

Establishment of stable cell lines expressing N-terminally FLAG-tagged MILL molecules and generation of rabbit antisera specific for MILL molecules

To facilitate biochemical analysis, we transfected FLAG-tagged expression plasmids into the mouse T lymphoma cell line RMA and established stable cell lines, RMA-MILL1 and RMA-MILL2, expressing N-terminally FLAG-tagged MILL1 and MILL2 molecules, respectively (Fig. 1*A*). Cell surface expression of MILL1 and MILL2 was confirmed by flow cytometry using the anti-FLAG Ab as well as the rabbit antisera generated against bacterially expressed MILL1 and MILL2 molecules. The specificity of our rabbit antisera was further confirmed by Western blot analysis of whole cell lysates (Fig. 1*B*). The anti-FLAG Ab detected two major bands of 48 and 41 kDa in RMA-MILL1 cells. The band of 41 kDa was nonspecific because it was detected in untransfected RMA cells. A major band of 48 kDa and a minor band of 44 kDa were detected by the anti-MILL1, but not anti-MILL2, antiserum (Fig. 1*B*). In RMA-MILL2 lysates, the anti-FLAG Ab detected bands of 43 and 41 kDa (Fig. 1*B*, *top*), which were also detected with the anti-MILL2, but not anti-MILL1, antiserum (Fig. 1*B*, *bottom*). Thus, the band of 41 kDa detected by the anti-FLAG Ab in RMA-MILL2 cells presumably represents doublets containing both specific and nonspecific signals. We also expressed MILL1 and MILL2 molecules on RMA cells using their endogenous signal peptides and performed cytometric analysis using the MILL-specific rabbit antisera. We obtained staining patterns similar to those shown in Fig. 1*A* (data not shown).

Deduced MILL1 and MILL2 molecules have three potential *N*-linked glycosylation sites, respectively (19). To examine glycosylation status, we isolated MILL molecules from the stable transfectants by immunoprecipitation with the anti-FLAG Ab, removed

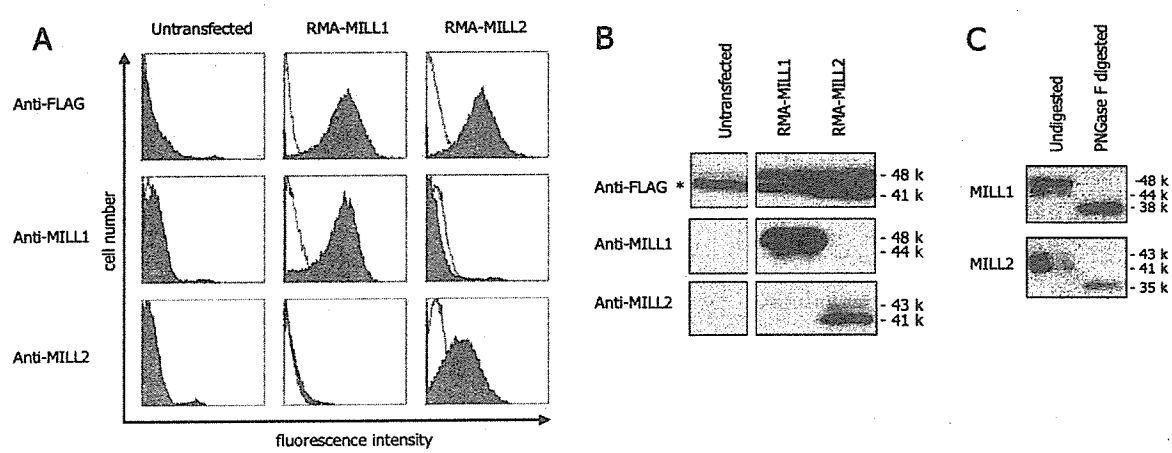

FIGURE 1. MILL1 and MILL2 are cell surface glycoproteins with *N*-linked sugars. *A*, Untransfected RMA cells and the transfected cell lines, RMA-MILL1 and RMA-MILL2, which stably express MILL1 and MILL2, respectively, were incubated with anti-FLAG mAb and FITC-conjugated goat anti-mouse IgG, anti-MILL1 antiserum (1/500 dilution) and FITC-labeled swine anti-rabbit Ig, or anti-MILL2 antiserum (1/500 dilution) and FITC-labeled swine anti-rabbit Ig (from the top to the bottom, shaded histograms). Negative control staining (open histograms) was obtained using an isotype-matched control Ab (top three panels) or normal rabbit serum (all other panels). Stained cells were analyzed by flow cytometry. *B*, Whole cell lysates of RMA-MILL1 and RMA-MILL2 were separated on 12% SDS-PAGE and subjected to immunoblotting using anti-FLAG mAb (top), anti-MILL1 antiserum (middle), or anti-MILL2 antiserum (bottom). Signals were detected by HRP-conjugated secondary Ab and ECL-Plus reagents. Nonspecific bands are indicated by asterisks. *C*, MILL1 and MILL2 proteins were immunoprecipitated with anti-FLAG mAb-coupled protein G-Sepharose beads from RMA-MILL1 and RMA-MILL2 cell lysates, respectively. After digestion with PNGase F at 37°C for 18 h, samples were separated on 12% SDS-PAGE and subjected to immunoblotting. MILL1 was detected by the rabbit anti-MILL1 antiserum and MILL2 by the rabbit anti-MILL2 antiserum. Signals were detected by HRP-conjugated secondary Ab and ECL-Plus reagents.

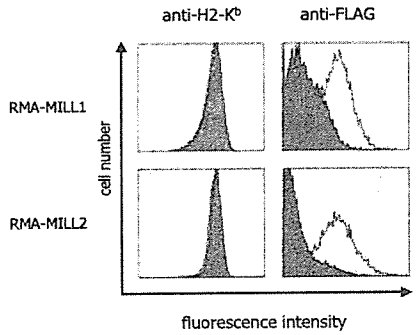

FIGURE 2. MILL1 and MILL2 are GPI-anchored proteins. RMA-MILL1 and RMA-MILL2 cells (top and bottom, respectively) were incubated with 1 U/ml PI-PLC (shaded histograms) or PBS (open histograms). Subsequently, cells were stained with anti-H2-K^b (left) or anti-FLAG (right) mAb. An FITC-conjugated F(ab')$_2$ fragment of goat anti-mouse IgG was used as a secondary Ab. Stained cells were analyzed by flow cytometry.

N-linked glycans with PNGase F and performed immunoblot analysis with the MILL-specific antisera (Fig. 1*C*). We obtained two bands of 44 and 48 kDa for non-treated MILL1, and a single band of 38 kDa for PNGase F-treated MILL1 (Fig. 1*C*, *top*). Similarly, we obtained two bands of 41 and 43 kDa for non-treated MILL2, and a single band of 35 kDa for PNGase F-treated MILL2 (Fig. 1*C*, *bottom*). The expression constructs used for stable transfection predicted M_r of 39280.83 and 35013.86 for the protein moieties of N-terminally flagged MILL1 and MILL2 molecules, respectively. Thus, the sizes of deglycosylated products agreed well with theoretical expectations. These results indicate that MILL1 and MILL2 are cell surface glycoproteins with *N*-linked sugars.

MILL1 and MILL2 are GPI-anchored proteins

We initially assumed that MILL1 and MILL2 were transmembrane proteins (19, 20). However, different prediction algorithms yielded inconsistent results concerning the presence or absence of transmembrane regions. Subsequent sequence analysis using the software 'big-PI Predictor' (25) suggested that MILL1 and MILL2 were likely GPI-anchored proteins. To examine this possibility, RMA-MILL1 and RMA-MILL2 cells were treated with PI-PLC, stained with the anti-FLAG Ab and examined by flow cytometry. In both RMA-MILL1 and RMA-MILL2 cells, cell surface staining was reduced markedly by PI-PLC treatment (Fig. 2, *right panel*). By contrast, cell surface staining with the H2-K^b Ab was not affected by similar treatment (Fig. 2, *left panel*), consistent with the fact that H2-K^b is an integral membrane protein. These results indicate that MILL1 and MILL2 are GPI-anchored cell surface proteins.

Cell surface expression of MILL molecules is TAP-independent

RMA-S is a variant derived from RMA cells (21) that lacks functional TAP molecules because of a defective TAP2 subunit (26, 27). At 37°C, classical class I molecules are barely expressed on the surface of RMA-S cells because empty class I molecules (class I molecules without peptides) are thermodynamically unstable. However, RMA-S cells express empty class I molecules when they are cultured at lower temperatures (28). To examine whether surface expression of MILL requires TAP, we transfected RMA-S cells with MILL expression plasmids and established stable transfectants. These cells were cultured at 25°C or 37°C and stained with the anti-FLAG or anti-H2-K^b Ab. As expected, endogenous H2-K^b molecules were expressed on RMA-S cells at the level comparable to that expressed on RMA cells when these cells were cultured at 25°C (Fig. 3, *A* and *B*, *left panel*, open histograms). However, expression of H2-K^b on RMA-S cells was reduced markedly when the cells were cultured at 37°C (Fig. 3, *A* and *B*, *left panel*, shaded histograms). By contrast, the expression levels of MILL1 and MILL2 detected by the anti-FLAG Ab were nearly the same regardless of whether the RMA-S cells were cultured at 25°C or 37°C (Fig. 3, *A* and *B*, *right panel*). These results indicate that cell surface expression of MILL molecules is TAP-independent.

Cell surface-expressed MILL1 and MILL2 molecules are associated with β_2m

To examine whether MILL molecules are associated with β_2m in vivo, we performed coimmunoprecipitation analysis. After treatment of RMA-MILL1 and RMA-MILL2 cells with PI-PLC, the MILL molecules released into the supernatants were immunoprecipitated with the anti-FLAG Ab and subjected to immunoblotting analysis using the anti-FLAG and anti-mouse β_2m Ab (Fig. 4). We found that β_2m was coimmunoprecipitated with both MILL1 and MILL2, indicating that MILL molecules are associated with β_2m on the cell surface.

β_2m facilitates the refolding of MILL molecules

To examine whether MILL1 and MILL2 can associate with β_2m in vitro, we expressed the extracellular domains of MILL1 and MILL2 in *E. coli* and refolded them in the presence or absence of mouse β_2m. MILL1 could be successfully refolded only in the presence of β_2m (Fig. 5*A*, *top panel*), and MILL1 and β_2m were eluted in the same fractions in gel filtration chromatography as revealed by SDS-PAGE analysis (Fig. 5*B*, *bottom half*, *top panel*). Although MILL2 was able to form soluble proteins when it was refolded in the absence of β_2m, β_2m appeared to improve the efficacy of refolding, consistent with our other results (Fig. 5*A*, *bottom panel*). MILL2 refolded in the presence of β_2m was eluted earlier in gel filtration chromatography than that refolded in the absence of β_2m (Fig. 5*A*, *bottom panel*), indicating that MILL2

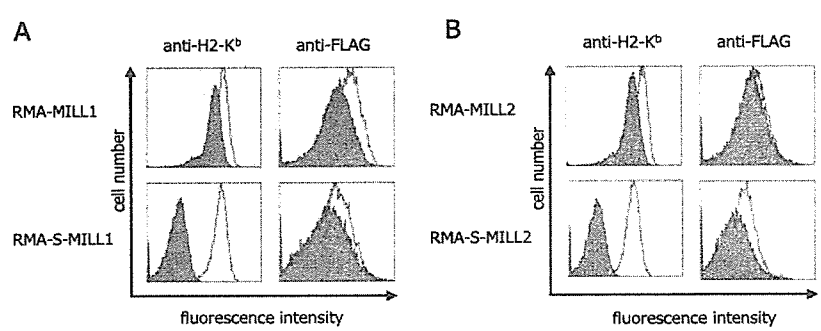

FIGURE 3. Cell surface expression of MILL molecules does not require functional TAP molecules. *A*, RMA-MILL1 and RMA-S-MILL1 cells were cultured at 25°C (open histograms) or 37°C (shaded histograms) for 18 h. Cells were incubated with anti-H2-K^b (left) or anti-FLAG (right) and then treated with FITC-conjugated F(ab')$_2$ fragments of goat anti-mouse IgG. Stained cells were analyzed by flow cytometry. *B*, RMA-MILL2 and RMA-S-MILL2 cells were treated in the same manner as in *A*, and cell surface expression of MILL2 was monitored by flow cytometry.

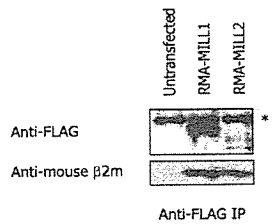

FIGURE 4. Cell surface-expressed MILL1 and MILL2 molecules are associated with β_2m. RMA-MILL1 and RMA-MILL2 cells were treated with PI-PLC and soluble MILL proteins were purified by immunoprecipitation with anti-FLAG mAb-coupled protein G-Sepharose beads (right). Precipitated samples were separated on 12% (top) or 14% (bottom) SDS-PAGE and subjected to immunoblotting analysis. MILL1 and MILL2 were detected by anti-FLAG mAb (top) whereas mouse β_2m was detected by anti-mouse β_2m Ab (bottom). Signals were detected by HRP-conjugated secondary Ab using the Super Signal West Dura kit. An asterisk indicates mouse IgG H chains.

molecules refolded in the presence of β_2m were associated with β_2m, which was further confirmed by SDS-PAGE analysis (Fig. 5*B*, *bottom panel*). MILL1 and MILL2 refolded in the presence of β_2m were purified by anion-exchange chromatography followed by gel filtration chromatography. The purified MILL1 and MILL2 proteins contained β_2m as a subunit (Fig. 5*C*). These results indicate that efficient refolding of MILL1 and MILL2 requires β_2m as a subunit. The molecular masses of MILL1/β_2m and MILL2/β_2m complexes estimated by gel filtration chromatography (Fig. 5*A*) and the relative intensities (3:1) of the MILL1 and MILL2 bands to the β_2m bands in the purified MILL1/β_2m and MILL2/β_2m complexes (Fig. 5*C*) indicate that the MILL1 or MILL2 polypeptide and β_2m bind at a 1:1 ratio.

MILL1 is expressed in a subpopulation of thymic medullary epithelial cells and a restricted region of inner root sheaths in hair follicles

To determine the tissue distribution of MILL1 and MILL2 molecules, we first performed Western blot analysis using the antisera for MILL1 and MILL2 against a panel of tissues isolated from adult and neonatal mice. These experiments yielded no bands in any tissues, presumably because the expression levels of MILL1 and MILL2 are low (data not shown). Our previous RT-PCR analysis (19) indicated that *Mill1* was transcribed in selected tissues including neonatal thymus and skin. We therefore examined expression of MILL1 in these tissues (Fig. 6). Staining was observed in a subpopulation of medullary epithelial cells in the neonatal thymus (Fig. 6*A*). These MILL1-positive cells were also detectable in the thymus of adult mice (data not shown). In the skin of 3-day-old mice, cells stained with the anti-MILL1 antiserum were found in the hair follicle (Fig. 6*B*, left). However, these cells became undetectable in the skin of 10-day-old (Fig. 6*B*, right) or 6-wk-old (not shown) mice. To more precisely address the locations of cells stained with the anti-MILL1 antiserum, we performed immunohistochemical staining of hair shafts and outer root sheaths (Fig. 6*C*). Cells stained with the anti-MILL1 antiserum were located outside the hair shaft (stained green with AE13 mAb), but inside the outer root sheath (stained green with AE1/AE3 mAb). Thus, positively stained cells are located in the inner root sheath. Because not all regions of inner root sheaths were stained with the antiserum, MILL1 seems to be expressed in a restricted region of the inner root sheath. To confirm the specificity of staining, we prepared anti-MILL1 antiserum preabsorbed with RMA-MILL1 or RMA cells. Preabsorption of the antiserum with RMA-MILL1 cells almost eliminated staining in thymic epithelial cells and hair follicles whereas staining was retained when the antiserum was preabsorbed with RMA cells (data not shown). *Mill2* is transcribed almost ubiquitously at low levels (19). We stained several tissues including neonatal thymus and skin as well as adult aorta, uterus, heart, kidney and spleen with the antiserum for MILL2 (1/200 dilution). Although this antiserum, when used at this dilution, was capable of staining RMA-MILL2 cells grown in vivo in C57BL/6 mice, we were unable to obtain any positive staining for MILL2 in any of the tissues (data not shown).

Cell surface expression of MILL1 on thymic epithelial cells requires β_2m

To examine whether cell surface expression of MILL1 requires β_2m, we isolated thymic stromal cells from 4-wk-old β_2m-deficient mice and stained with the anti-MILL1 antiserum (Fig. 7). Cell surface expression of MILL1 was almost completely abrogated in the β_2m-deficient mice compared with the adult C57BL/6 mice, indicating that cell surface expression of MILL1 is β_2m-dependent.

Discussion

MILL is the latest addition to the growing list of mammalian MHC class I families encoded outside the MHC region. Our previous work has revealed several unique features of this class I family (19, 20). First, not all mammalian species have the MILL family; although mice and rats have this family, it is absent in humans. Because MILL apparently arose before the radiation of mammals, humans seem to have lost this class I family. Second, unlike all other class I genes, the genes coding for mouse MILL have an exon between those coding for the signal peptide and the α1 domain. Third, the MILL family is phylogenetically most closely related to the MICA/B family among known class I families. Because the MILL family is absent in humans, and conversely, mice and rats lack the MICA/B family, we suggested that MILL might serve as a functional substitute of MICA/B in rodents (19). Fourth, deduced MILL molecules lack most of the residues required for the docking of peptide termini, suggesting that they are unlikely to bind peptides. Fifth, RT-PCR analysis indicated that the members of the MILL family are poorly transcribed in most adult tissues, suggesting a role other than conventional Ag presentation. Sixth, sequence comparison of rat and mouse MILL molecules revealed that *Mill* is one of the most rapidly evolving class I gene families, and that, in both *Mill1* and *Mill2*, non-synonymous substitutions occur more frequently than synonymous substitutions in the α1 domain whereas the opposite is the case in the α2 and α3 domains, suggesting that the α1 domain may be under positive selection (20). Taking all of these points into consideration, we suggested that MILL may perform specialized immune functions required only in certain species or some redundant functions, part of which are executed by other molecules (20).

In the present study, we set out to perform a biochemical characterization of mouse MILL molecules. Consistent with the absence of key residues required for the docking of peptides, we found that cell surface expression of MILL1 and MILL2 does not require functional TAP molecules (Fig. 3). Furthermore, the extracellular domains of MILL1 and MILL2 expressed in *E. coli* could be efficiently refolded in the absence of peptides under standard class I refolding conditions when β_2m was added into the mixture (Fig. 5). This is in contrast to the fact that refolding of recombinant class Ia molecules isolated from purified bacterial inclusion bodies requires the presence of a peptide ligand and is reminiscent of the behaviors of certain class Ib molecules, the refolding of which is ligand-independent (29–31). Taken together, it